AD_____

Award Number: DAMD17-99-1-9250

TITLE: Expression Profiling of Tyrosine Kinase Genes

PRINCIPAL INVESTIGATOR: Heinz-Ulrich Weier, Ph.D.

CONTRACTING ORGANIZATION: University of California at Berkeley
                           Berkeley, California 94720

REPORT DATE: August 2001

TYPE OF REPORT: Annual

PREPARED FOR: U.S. Army Medical Research and Materiel Command
               Fort Detrick, Maryland 21702-5012

DISTRIBUTION STATEMENT:
Approved for public release; distribution unlimited

The views, opinions and/or findings contained in this report are
those of the author(s) and should not be construed as an official
Department of the Army position, policy or decision unless so
designated by other documentation.

20020719 098

REPORT DOCUMENTATION PAGE	Form Approved OMB No. 074-0188

Public reporting burden for this collection of information is estimated to average 1 hour per response, including the time for reviewing instructions, searching existing data sources, gathering and maintaining the data needed, and completing and reviewing this collection of information. Send comments regarding this burden estimate or any other aspect of this collection of information, including suggestions for reducing this burden to Washington Headquarters Services, Directorate for Information Operations and Reports, 1215 Jefferson Davis Highway, Suite 1204, Arlington, VA 22202-4302, and to the Office of Management and Budget, Paperwork Reduction Project (0704-0188), Washington, DC 20503

1. AGENCY USE ONLY (Leave blank)	2. REPORT DATE August 2001	3. REPORT TYPE AND DATES COVERED Annual (1 Aug 00 - 31 Jul 01)

4. TITLE AND SUBTITLE
Expression Profiling of Tyrosine Kinase Genes

5. FUNDING NUMBERS
DAMD17-99-1-9250

6. AUTHOR(S)
Heinz-Ulrich Weier, Ph.D.

7. PERFORMING ORGANIZATION NAME(S) AND ADDRESS(ES)

University of California at Berkeley
Berkeley, California 94720

E-Mail: UGWeier@lbl.gov

8. PERFORMING ORGANIZATION REPORT NUMBER

9. SPONSORING / MONITORING AGENCY NAME(S) AND ADDRESS(ES)

U.S. Army Medical Research and Materiel Command
Fort Detrick, Maryland 21702-5012

10. SPONSORING / MONITORING AGENCY REPORT NUMBER

11. SUPPLEMENTARY NOTES
report contains color

12a. DISTRIBUTION / AVAILABILITY STATEMENT

Approved for public release; distribution unlimited

12b. DISTRIBUTION CODE

13. ABSTRACT (Maximum 200 Words)

e expression of genes involved in signal transduction (e.g. protein kinases) is often ed in tumors. The aberrant expression of several of these genes typically parallels rogression toward a more malignant phenotype. We developed a cDNA micro-array – based ling system to measure the level of expression of tyrosine kinase (tk) genes. The are for preparation of cDNA micro-arrays and basic protocols for hybridization were ped in year 1. In the second year, we finished isolating RNA and cDNA synthesis from ast cancer cell lines and 10 frozen tissues. We optimized protocols for tk-specific plification and cloning. We continued our DNA sequencing effort and added additional s to our micro-arrays. Using well-characterized breast cancer cell lines, the system red reproducible results about tk gene expression during cell transformation and ssion toward a more malignant phenotype. Comparing the absolute expression levels DNA micro-arrays with data from Northern blot analyses suggested that our initial ch using mixed-based oligonucleotide primers led to lowered representation of highly nt transcripts. This problem will be addressed with a new primer design in the ng year when we will investigate the tk gene expression in small samples.

14. SUBJECT TERMS
Breast Cancer, gene expression, tyrosine kinase

15. NUMBER OF PAGES
46

16. PRICE CODE

17. SECURITY CLASSIFICATION OF REPORT	18. SECURITY CLASSIFICATION OF THIS PAGE	19. SECURITY CLASSIFICATION OF ABSTRACT	20. LIMITATION OF ABSTRACT
Unclassified	Unclassified	Unclassified	Unlimited

NSN 7540-01-280-5500

Standard Form 298 (Rev. 2-89)
Prescribed by ANSI Std. Z39-18
298-102

Table of Contents

INTRODUCTION:

Aberrant expression of receptor or cytosolic tyrosine kinase genes and, in particular, their hyper-expression are common phenomena in breast cancer, which are believed to alter cell growth and response to external signals such as growth factors, hormones etc. Knowledge about the relative levels of expression of many tyrosine kinase genes, all at the same time, might contribute significantly to a better understanding of the processes of tumor development and progression. We are developing a rapid assay that will use innovative cDNA micro-arrays carrying small amounts of individual tyrosine kinase gene-specific targets to simultaneously determine the expression levels of up to 100 tyrosine kinase genes using a small number of cells. Three years of research and development will lead to discovery of a set of gene-specific markers associated with breast cancer progression and a simple device capable of performing inexpensive expression profiling of these markers. The research and development efforts in the first year of this 3-year project focused on the design and testing of robotic instruments to prepare DNA micro-arrays and the preparation of prototype arrays carrying sets of more than 50 gene-specific tyrosine kinase fragments. The second year effort (i.e., the reporting period 1 Aug 00 –31 Jul 01) was directed towards the optimization of cDNA preparation, labeling, hybridization and detection protocols as well as the molecular cloning and sequencing of breast cancer-specific tyrosine kinase gene transcripts.

BODY:

Here, we report our progress as it relates to the approved 'Statement of Work'.

***Task 1.* Identify tyrosine kinase (tk) genes expressed in normal and neoplastic breast tissues**

    1.1 Prepare cDNAs from ten cell lines and ten frozen tissue specimens (months 1-18)

We isolated total RNA from 16 different breast cell lines and ten frozen tissue specimens. Exponentially growing cell lines or isolated RNA's were provided to us by the following collaborators:

Paul Yaswen, Ph.D., Martha Stampfer, Ph.D., Daniel Callahan, Ph.D., and Ruth Lupo, Ph.D., from LBNL, and Chris Benz, M.D., from the Buck Institute for Aging Research, Novato, CA. The actual number of cell lines or RNA's provided is higher, because we processed several aliquots of what is believed the same cell line. For example, we received MCF-7 cells from D. Callahan and MCF-7 RNA from P. Yaswen and C. Benz.

Table I. Breast cancer cell lines used in our experiments.

ZR75	SKBR3
BT474	BT468
BT549	MCF-7
184A1	184A1TH-6
184B5	184B5-ME
T47D	MDA-MB-453
MDA-MB-436 plus Vit. A	MDA-MB-436 plus pCMr3.1
600MPE	HMEC

Normal breast tissue and breast cancer tissue specimens were obtained from the University of California Comprehensive Cancer Center (Joe W. Gray, Ph.D., B.M. Ljung, M.D. and K. Chew). We received a total of 10 frozen tissue specimens representing 3 normal tissues and 7 cancer tissues. RNA was extracted using a commercial kit (Qiagen) and transcribed into cDNA immediately after isolation. Remaining RNA was stored at –80 degrees.

We prepared cDNAs from the RNA by random priming and reverse transcription. The names of the various cell lines are shown in Table I. Commercial kits (Qiagen, Roche, Ambion) were used for all steps. Typically, 1 μg of total RNA produced sufficient quantities of cDNA for cloning and/or repeated micro-array analyses.

1.2 Perform RT-PCR reactions and clone PCR products in plasmids (months 3-18)

We used about 100 ng of DNA in PCR reactions to amplify tk-specific cDNA fragments with our mixed-base F-/R-TYRK primers. PCR amplification was performed for 35 cycles using mixed base primers that bind to the conserved sequences of domains VII and IX of the tyrosine kinase genes (F-TYRK: 5'-GGGCGTCAGAARRTNRSNGAYTTYGG-3'; R-TYRK: 5'-GCGCGGGCC-CRWANSHCCANACRTCNSA-3'). Each cycle consisted of a denaturation step of 30 sec at 94°C, primer annealing at 53°C for 60 sec and primer extension for 120 sec at 72°C. Most PCR products appeared as a single broad band of the expected size (~160-170 bp). The amplification products were separated on a 4% agarose gel, and a slice containing fragments of approximately 160-180 bp was excised. The gel slice was rinsed with water and melted by heating in 100 μl water. About 2 μl of this solution was transferred to 200 μl of PCR buffer containing the modified F-TYRK/R-TYRK primers designed to include deoxy-UMP residues and a Not I restriction site at their respective 5'-ends (F-TYRKU: 5'-CUACUACUACUAGCGGCCGCAARRTNRSNGAYTTYGG-3'; R-TYRK: 5'-CAUCAUCAUCAUGCGGCCGCCCRWANSHCCANACRTCNS-3'). This gave PCR products of the expected size (about 190 bp) suitable for treatment with Uracil DNA Glycosylase (UDG) and cloning into pAMP1 (Gibco/LTI). Transformation was performed using MAX Efficiency DH5a competent cells (Gibco/LTI). Cells were incubated overnight at 37°C on LB plates containing 100μg/ml ampicillin, 50μg/ml X-gal, and 1mM IPTG (Gibco/LTI). Ampicillin resistant clones were picked from agar plates and their insert sizes were determined by agarose gel analysis of PCR products generated with vector-specific PCR primers.

1.3 Perform pre-screening with known tk fragments, cDNA sequencing and database searches (months 5-22)

The DNA from plasmid clones with inserts of about 125-190 bp was isolated, fingerprinted or screened against known tk genes, and 'novel' clones were sequenced at the UC Berkeley, Biochemical Core Facility. The list of genes cloned and identified so far contained several sequences reported to have transforming activity, such as trk, axl/ufo or to be overexpressed in various types of cancer. Our present panel of kinase gene tags used to prepare cDNA micro-arrays contains 60 genes among them four novel sequences and HLA-A, which happens to be amplified by our PCR primers. In the reporting period, we noticed an elevated fraction of clones that were sequenced and revealed a previously sequenced insert, suggesting that our pre-screening procedure was not sufficiently stringent. For example, one batch sequencing procedure of 20 plasmid clones showed previously identified tk fragments in 18 out of 20 reaction, while the remaining 2 clones contained novel sequences without matches in the Genbank database.

1.4 Add novel clones to the panel of expressed tk gene fragments (months 6-24)

As of June 2001, we cloned and partially characterized about 240 tk fragment containing plasmid clones derived from breast cancer tissues and cell lines. These clones join more than 500 tk fragments containing clones that were previously isolated from thyroid and prostate tumors. From these clones, DNA was isolated, bound to nylon filters and prescreened with probes prepared from known tk clones. Following this pre-screening step, we performed cDNA sequencing and database searches. In about 100 tk containing plasmids that were sequenced, we found two potentially novel tk genes. The other sequenced clones contained two known kinases that we added to our panel. The remaining clones contained sequences that were already part of the panel suggesting insufficioent stringency during the pre-screening process. At this point we decided to focus our efforts on the optimization of the PCR amplification (see 2.3, below). And added novel clones to the panel of expressed tk gene fragments. DNA isolated from this panel of tk gene fragments is then arrayed and printed onto glass slides to measure tk gene expression in cell lines, normal tissues, and tumor tissues.

We initiated a search for full length cDNA clones for some of the novel tk sequences found expressed in breast cancer. We will hire a local company (Pangene of Fremont, CA) to screen the proprietary cDNA libraries for full length clones.

Task 2. Measure tk gene expression in cell lines, normal and tumor tissues
2.1 Prepare DNA microarrays carrying about 100 different sequences (months 3-24)

The fabrication of tyrosine kinase (tk) cDNA arrays on glass slides was done in house using the laboratory-built robotic system to print cDNA micro- arrays with about 124 target spots per array. The arrayer can print up to 91 slides in a single run. Routinely, we print approximately 50 slides per run, with duplicate arrays on each slide. The stainless steel printing pin has an open slit in the tip. Each loading takes up approximately 1 µl of DNA solution and allows continuous printing of more than 100 dots. A full 384-well plate of DNA samples can be arrayed onto 50 slides (in duplicate) in 8 hrs, including the time needed for repeated wash and drying steps in each printing cycle. We concentrated our PCR products and dissolved DNA in 50% dimethyl sulfoxide (DMSO) at a concentration of 250ng/µl. Spot diameters on poly-L-lysine coated slides ranged from 80-125 µm. The arrayer has a positioning precision of approximately 15µm, therefore, an array with 200µm center-to-center distance between spots is sufficiently spaced.

Standard microscope glass slides were cleaned thoroughly with concentrated sodium hydroxide and ethanol before being coated with poly-L-lysine. These steps provided a positively charged layer to bind DNA to the slides. The coated slides were stored in ambient air in closed slide boxes two weeks before they were used for printing. The locations of arrays were marked on the reverse side of the slides with diamond marker pen. The slides were placed upside down in a chamber filled with 1x SSC and re-hydrated for 5 to 15 minutes (depending on the size of the array). Spots are not allowed to swell too much and run into each other. Hydrated slides were dried on a hot plate set to 70 °C for 3 seconds. These slides were then UV cross-linked using a Stratalinker 1800 (Stratagene) set to 65 mJ. Following cross-linking, slides were incubated in blocking solution (0.21M succinic anhydride in 1-methyl-2-pyrrolidinone, 0.06M sodium borate for 20 minutes (pH 8.0)). The slides were then denatured in boiling water for 2 min, and submerged in 95% ethanol for 1 minute. After a centrifugation at 500 rpm for 5 min to remove traces of ethanol or water, the arrays were ready for hybridization or storage.

Quality control for the tk arrays was monitored throughout the tk array fabrication process. All

reagents used for printing and coating of slides were prepared fresh and filtered. Before post-printing processing of the arrays, morphology of the spot and DNA distribution within the spots were examined with DAPI staining and visualized in a Zeiss fluorescence microscope. After post-printing processing, arrays were stained with POPO-3 dye (0.01 mM) and scanned at Cy3 channel to ensure the retention of DNA on the arrays for hybridization.

2.2 Optimize hybridization conditions to provide quantitative information (months 6-24)

We isolated total RNA from breast cancer cell lines or frozen tissues sections. We then prepared cDNAs from the RNA by random priming and reverse transcription using commercial kits (Qiagen, Roche, Ambion). Typically 1 μg of total RNA can produce sufficient quantities of probe for all microarray analyses. We used about 100 ng of cDNA in PCR reactions to amplify tk-specific cDNA fragments with our mixed-base F-/R-TYRK primers. Following 30 cycles of PCR, the amplification products were separated on a 4% agarose gel stained with ethidium bromide, and a slice that contained fragments of approximately 160-180 bp was excised. The gel slice was rinsed with water and melted by heating in 100 μl water. About 2 μl of this solution was transferred to 200 μl of PCR buffer containing the F-/R-TYRK primers. The tk fragments were then amplified a second time and the products concentrated via isopropanol precipitation. The tk fragments (about 400-600 ng per reaction (Hsieh et al. 2001)) were then labeled with either Cy3-dUTP (red fluorescence, shown green in the figures) or Cy5-dUTP (infrared fluorescence, shown red in the figures) by random priming (Life Technologies).

We optimized hybridization and wash conditions to obtain specificity and reduce background fluorescence to the level in which quantitative information could be obtained reproducibly. Slides were placed inside hybridization chambers with a cover fastened tightly by clamps. Multiple drops of 3X SSC were added around the arrays on the slide to maintain the humidity and prevent drying of hybridization solution. Hybridization was then performed under glass coverslips overnight at 65 ^{0}C. Next day, the arrays were then washed in 3 changes of wash solution (1x SSC+ 0.03% SDS) at room temperature for 5 minutes, 0.2x SSC at room temperature for 1 minute, and then 0.2x SSC at 50 ^{0}C for 1 minute. After the washes, the slides were dried immediately by centrifugation at 500 rpm for 5 min before scanning. Current sample preparation and hybridization procedures have produced signal to background (noise) ratios of more than 100 (in the green channel) to more than 200 (in the red channel).

The performance of the system was tested by hybridization of fluorochrome-labeled tk gene-specific PCR fragments onto our tk-specific DNA micro-arrays. In preliminary experiments, we used a first generation of DNA micro-arrays comprised of 48 kinase genes previously identified to be expressed in thyroid tumors (not shown). This allowed us to optimize hybridization and wash conditions. We then prepared DNA micro-arrays carrying a more extensive panel of tk genes plus a few control genes (Table II. We found that hybridization to these arrays (Figure 1) provided reproducible information relevant to tumor progression and differences between cell lines. For some of our experiments, we want to compare the expression levels of tk genes in a tissue sample against a constant standard rather than against a second tissue sample. Here, the small size of our array is an advantage. We can readily create a reference standard to compare tk expression in a given tissue simply by making a cocktail containing equimolar amounts of each tk spot on the array. This artificial cocktail mix of DNAs is then labeled by random priming with Cy3-dUTP or Cy3-dUTP in an identical manner as the cDNAs derived from mRNA.

2.3 Optimize PCR parameters for quantitative amplification of target genes (months 12-18)

We have worked out an effective method to generate probe for our microarray experiments. In our original method, we isolate total RNA from frozen tissues cell lines and prepared cDNAs from the RNA by random priming and reverse transcription, before we amplify tk-specific cDNA fragments with our mixed-base F-/R-TYRK primers.

In the course of our experiments, we have discovered that this probe synthesis method can generate quality microarray data. This method is particularly good at assaying the expression of tk genes that are poorly or moderately expressed. We subjected our results to independent validations with colleagues expert in the expression of tk genes in the breast cells. We have the learned that our original method seems to recapitulate the results of other investigators (using Northern blots) for moderate and low expressing tk genes. However, we have also learned that highly expressed tk gene expression is less accurately represented in our experiments than we would prefer. The rank ordering of the high expressing genes is maintained (i.e. for tk genes that are highly expressed, a lower-expressed tk gene indeed appears to be expressed less than a higher-expressed tk genes). However, the apparent difference between highly expressed genes are less than one might expect. In essence, our original probe synthesis scheme is not completely representative of total tk expression.

We believe that the cause of this artifact is due to the depletion of degenerate primers in the early steps of PCR synthesis. Our degenerate primer mixes contain equimolar concentrations of each of the hundreds of different primers. Of course, the population of tk RNAs within and tissues sample is likely to be anything but equimolar. It is probable that the most highly expressing genes are rapidly depleting the population of degenerate primers that would be perfect matches for that species. Once perfect primers are depleted, sub-optimal primers then bind with baspair mismatches leading to degrade PCR performance.

We are currently testing revised methods to eliminate this problem. Our new PCR scheme utilizes new degenerate tk primers that have an unrelated 18-25 bp adapter sequence at its 5'-end and the tk –specific sequence on its 3'-end. The previous work of Eberwine (Eberwine, 1996) with a T7 adaptor sequence for in vitro transcription suggested that M13 or T7/T3 primer sequences on the 5'-ends should work well. The new degenerate primers are used for only a handful of PCR cycles with the cDNAs to initiate the amplification of the tk sequences. Then the degenerate primers are removed with a spin column, and the adapter primers (representing the non-degenerate 5'-ends) are added to the products of the first PCR reaction. The adapter primers then complete the reaction. By allowing the degenerate primers access to our cDNA for only a very few cycles, we believe we can make our microarray results more representative. This will be even more important as we move to smaller samples sizes. We have already tested different adaptor sequences, and are now in the process to compare the complexity of PCR products generated with either to old or the new amplification strategy.
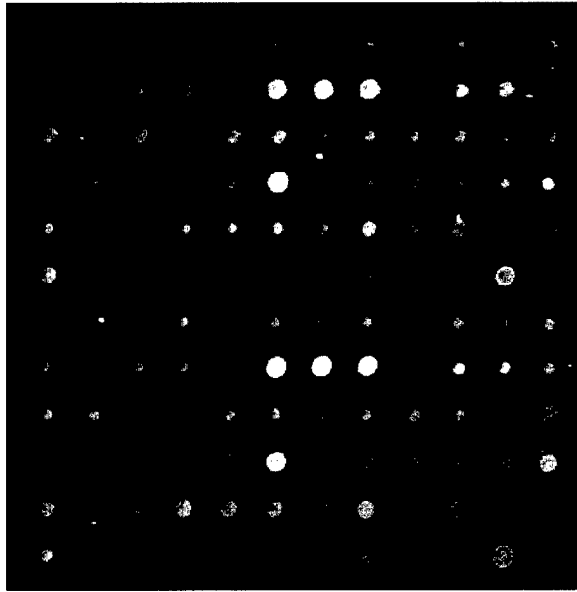
Figure 1: Results of hybridization of CY3-labeled tk DNA fragments from breast cancer cell line 184A1 (shown in green) in combination with CY5 –labeled TK fragments from normal breast tissue (shown in red) reveals specific differences in the expression of tk genes.

	1	2	3	4	5	6	7	8	9	10	11	12
1	GAPDH	HPRT	RPL13A	K-SAM	c-mer	CLK3	flg	HSIGFIR R	blk	c-src	EphA2	EphA4
2	HSLK/KI AA0204	PTK6	c-syn/FYN	EGFR	HLA-A	HSUO7349	c-abl	c-yes-1	blk-like	EphA1	EphB4	c-fms
3	pkC-delta	fer	HSEGF01	HUMP4K	HUMPKS CD	JAK3	MKK3	RON	tyk2	EphA4	lck	MLK-3
4	TEK	TYRO3	ZAP-70	LYN	EphB1	UFO	IRR	MEK3	PDGF	tie	arg	JAK1
5	met	PYK2/FAK2	DRR1	MKK3	pra src pp60	clk1	MAPK1	no match	serium inducible	v-abl	Ste20-like	cosmid B1E7
6	G-protein-coupled	GAPDH	HPRT	RPL13A	TRK	ret (PTC3)	EphA2	ret (PTC3)	ret (HHCC55	TRK	erbB2	EphB2
7	GAPDH	HPRT	RPL13A	K-SAM	c-mer	CLK3	flg	HSIGFIR R	blk	c-src	EphA2	EphA4
8	HSLK/KI AA0204	PTK6	c-syn/FYN	EGFR	HLA-A	HSUO7349	c-abl	c-yes-1	blk-like	EphA1	EphB4	c-fms
9	pkC-delta	fer	HSEGF01	HUMP4K	HUMPKS CD	JAK3	MKK3	RON	tyk2	EphA4	lck	MLK-3
10	TEK	TYRO3	ZAP-70	LYN	EphB1	UFO	IRR	MEK3	PDGF	tie	arg	JAK1
11	met	PYK2/FAK2	DRR1	MKK3	pra src pp60	clk1	MAPK1	no match	serium inducible	v-abl	Ste20-like	cosmid B1E7
12	G-protein-coupled	GAPDH	HPRT	RPL13A	TRK	ret (PTC3)	EphA2	ret (PTC3)	ret (HHCC55	TRK	erbB2	EphB2

Table II: The organization of our new tk DNA microarrays used in studies of gene expression in breast cancer cell lines and tissue specimens.

2.4 Develop algorithms for array readout and comparisions between measurements (months 9-24)

A Axon GenePix 4000 (Axon Inc.) array scanner used to acquire all images has a preview resolution of 40 µm and a scanning resolution of 10 µm. The photomultiplier sensitivity can be adjusted by the user during preview to optimize the signal intensity. GenePix 3.0 (Axon Inc.), an image acquisition and analysis software, was used to analyze the images acquired from our tk arrays and provided numerical data that was imported into spreadsheets (Microsoft Excel) for further analysis. For display purposes, the images were saved in standard formats and imported into common graphics programs such as Adobe Photoshop. Given the relatively small numbers of arrays that have been hybridized so far, it was sufficient to normalize the data and compare numeric values in spreadsheets.

Task 3. Validate assays for multigene expression profiling in small amounts of tissue

3.1 Develop software for databasing, automated analysis of expression profile datasets and their annotation (months 18-24)

The GenePix software provides the results as numeric data that can be inported into spreadsheets or databases. We installed Microsoft Access software which will be sufficient to handle most or all of our databasing needs. We also installed BRB ArrayTools Version 1.03 recently released by the Biometric Research Branch of the Division of Cancer Treatment and Diagnosis at NCI. This package developed by Richard Simon and Amy Peng allows for a more comprehensive analysis of DNA microarrays and their annotation. The software is presently being tested using the datasets obtained with our second generation tk cDNA arrays.

KEY RESEARCH ACCOMPLISHMENTS:

- Finished the isolation of RNA and preparation of cDNA from 16 breast cancer cell lines and 10 frozen tissue specimens
- Completed the PCR-amplification of tk-specific DNA fragments and cloned the products into plasmids
- Pre-screening more than 400 breast cancer cell line-derived clones and sequenced an additional 100 clones, database searches identified two clones containing potentially novel tyrosine kinase genes
- Expanded the panel of tyrosine kinase genes used for expression profiling and printed second generation cDNA micro-arrays
- Generated artificial mixtures of tk DNA fragments to be used as reference DNA
- Reconfirmed tk gene expression changes as breast epithelial cells become tumorigenic and grow anchorage-independent using second generation tk micro-arrays
- Initiated search for full length cDNA clones for novel tk genes

REPORTABLE OUTCOMES:

- **manuscripts**

1. Hsieh H-B, Lersch RA, Callahan DE, Hayward S, Wong M, Clark OH, Weier H-UG (2001) Monitoring signal transduction in cancer: cDNA microarray for semi-quantitative analysis. J Histochem Cytochem 49: 1057-1058

2. Lersch RA, Fung J, Hsieh H-B, Smida J, Weier H-UG (2001) Monitoring signal transduction in cancer: from chips to FISH. J Histochem Cytochem 49:925-926

3. Weier H-UG, Zitzelsberger HF, Hsieh H-B, Sun MV, Wong M, Lersch RA, Yaswen P, Smida J, Kuschnick C, Clark OH (2001) Monitoring signal transduction in cancer: tyrosine kinase gene expression profiling. J Histochem Cytochem 49:673-674

4. Weier H-UG, Munné S, Lersch RA, Hsieh HB, Smida J, Chen XN, Korenberg JR, Pedersen RA, Fung J (2001) Towards a Full Karyotype Screening of Interphase Cells: 'FISH and Chip' Technology. Molecular and Cellular Endocrinology (in press)

5. Zitzelsberger H, Bruch J, Smida J, Hieber L, Peddie CM, Bryant PE, Riches AC, Fung J, Weier HUG, Bauchinger M (2001) Clonal chromosomal aberrations in simian virus 40-transfected human thyroid cells and in derived tumors developed after in vitro irradiation. Int J Cancer 96:166-177

6. Weier H-UG (2001) DNA Fiber Mapping Techniques for the Assembly of High-resolution Physical Maps. J Histochem Cytochem 49:939-948

- **poster presentations**

7. Hsieh, H.B., Weier, H.-U. G. Kinase Gene Expression Profiling by FISH and Chips. 11th International Congress of Histochemistry and Cytochemistry (ICHC 2000), York, UK, September 3-8, 2000.

8. Hsieh H-B, Lersch RA, Callahan DE, Hayward S, Wong M, Clark OH, Weier H-UG (2001) Monitoring signal transduction in cancer: DNA microarray for semi-quantitative analysis. 2001 Annual Meeting of the Histochemical Society, February 3-6, 2001, Santa Fe, NM.

9. Lersch RA, Fung J, Hsieh H-B, Smida J, Weier H-UG(2001) Monitoring signal transduction in cancer: from chips to FISH. 2001 Annual Meeting of the Histochemical Society, February 3-6, 2001, Santa Fe, NM.

10. Weier H-UG, Zitzelsberger HF, Hsieh H-B, Sun MV, Wong M, Lersch RA, Yaswen P, Smida J, Kuschnick C, Clark OH (2001) Monitoring signal transduction in cancer: tyrosine kinase gene expression profiling. 2001 Annual Meeting of the Histochemical Society, February 3-6, 2001, Santa Fe, NM.

CONCLUSIONS:

This 3-year IDEA project is well on track and, has met its initial milestones. The soft- and hardware components necessary for these studies were put in place in the first year. The results obtained with RNA isolated from cell lines and breast tissues have proven the hypothesis that changes in tk gene expression can be monitored by a combination of PCR using tk gene family-specific primers and DNA micro-arrays. While the hybridization to the DNA micro-array appears to possess the required specificity, second year research addressed the issues of hybridization background reduction and definition of a suitable reference DNA probe. Comparison of the cDNA micro-array data with those obtained by Southern blot analyses suggests a non-homogeneous amplification of tk fragments. This is now addressed by an altered PCR protocol involving new primers. Concordant with the timeline presented in the original proposal, research and development in the third year will focus on application of the technology to small numbers of cells.

REFERENCES:

Eberwine J (1996) Amplification of mRNA populations using aRNA generated from immobilized oligo(dt)-T7 primed cDNA. Biotechniques 20:584-591.

Hsieh H-B, Lersch RA, Callahan DE, Hayward S, Wong M, Clark OH, Weier H-UG (2001) Monitoring signal transduction in cancer: cDNA microarray for semi-quantitative analysis. J Histochem Cytochem 49: 1057-1058

APPENDICES:

1. Hsieh H-B, Lersch RA, Callahan DE, Hayward S, Wong M, Clark OH, Weier H-UG (2001) Monitoring signal transduction in cancer: DNA microarray for semi-quantitative analysis. J Histochem Cytochem 49: 1057-1058

2. Lersch RA, Fung J, Hsieh H-B, Smida J, Weier H-UG(2001) Monitoring signal transduction in cancer: from chips to FISH. J Histochem Cytochem 49:925-926

3. Weier H-UG, Zitzelsberger HF, Hsieh H-B, Sun MV, Wong M, Lersch RA, Yaswen P, Smida J, Kuschnick C, Clark OH (2001) Monitoring signal transduction in cancer: tyrosine kinase gene expression profiling. J Histochem Cytochem 49:673-674

4. Weier, H.-U.G., Munné, S., Lersch, R.A., Hsieh, H.B., Smida, J., Chen, X.N, Korenberg, J.R., Pedersen, R.A., Fung J. (2000) Towards a Full Karyotype Screening of Interphase Cells: 'FISH and Chip' Technology. Molecular and Cellular Endocrinology (in press)

5. Zitzelsberger H, Bruch J, Smida J, Hieber L, Peddie CM, Bryant PE, Riches AC, Fung J, Weier HUG, Bauchinger M (2001) Clonal chromosomal aberrations in simian virus 40-transfected human thyroid cells and in derived tumors developed after in vitro irradiation. Int J Cancer 96:166-177

6. Weier H-UG (2001) DNA Fiber Mapping Techniques for the Assembly of High-resolution Physical Maps. J Histochem Cytochem 49:939-948

Appendix 1

BRIEF REPORT

Monitoring Signal Transduction in Cancer: cDNA Microarray for Semiquantitative Analysis

H.-Ben Hsieh, Robert A. Lersch, Daniel E. Callahan, Simon Hayward, Mariwil Wong, Orlo H. Clark, and Heinz-Ulrich G. Weier

Life Sciences Division, Lawrence Berkeley National Laboratory, Berkeley, California (H-BH,RAL,DEC,H-UGW), and Departments of Urology (SH) and Surgery (MW,OHC), University of California–San Francisco, San Francisco, California

SUMMARY   This study targeted the development of a novel microarray tool to allow rapid determination of the expression levels of 58 different tyrosine kinase (tk) genes in small tumor samples. The goals were to define a reference probe for multi-sample comparison and to investigate the variability and reproducibility of the image acquisition and RT-PCR procedures. The small number of tk genes on our arrays enabled us to define a reference probe by artificially mixing all genes on the arrays. Such a probe provided contrast reference for comparative hybridization of control and sample DNA and enabled cross-comparison of more than two samples against one another. Comparison of signals generated from multiple scanning eliminated the concern of photo bleaching and scanner intrinsic noise. Tests performed with breast, thyroid, and prostate cancer samples yielded distinctive patterns and suggest the feasibility of our approach. Repeated experiments indicated reproducibility of such arrays. Up- or downregulated genes identified by this rapid screening are now being investigated with techniques such as in situ hybridization.

(J Histochem Cytochem 49:1057–1058, 2001)

OUR DNA microarray experiments followed the Brown laboratory's protocols (http://cmgm.stanford.edu/pbrown/mguide/index.html) with modifications on microarrayer construction and the following: spotted DNAs are homogeneous (270–290 bp); RNAs were amplified by RT-PCR with mixed-base tk primers, size-selected by electrophoresis (180–210 bp), and labeled by random prime reaction. Typical cDNA microarray experiments utilize two-color hybridization in which Cy5-labeled sample is hybridized against Cy3-labeled control to the same arrays (Schena 1996). This provides a convenient means to look at two treatment effects, such as two time points (Iyer et al. 1999) or tumor vs normal tissues (DeRisi et al. 1996). However, when multiple samples are to be compared against one another, pair-wise comparisons are inefficient. To address such needs and reduce the complexity, a "standard" or "reference" probe is preferred. Because the hybridiza-

tion is competitive with limited labeled DNA (Cheung et al. 1999), a pooled mixture that represents all genes at low (but detectable) levels will be an ideal reference. For large-format cDNA microarray, pooled mixtures of several normal tissues or cell lines were used (Celis et al. 2000). Such pools of RNA can vary from preparation to preparation, and highly expressed genes can skew or saturate the arrays. With a small number (58) of genes on our tk arrays, we were able to artificially mix individual genes proportionally and to amplify them in large quantity for a particular project. Pair-wise hybridizations with this reference probe have yielded similar results that proved this approach feasible.

To test the extent of the scanner's intrinsic noise, slides were scanned 12 times repeatedly at full laser power. Four separate pixels belonging to four intensity groups were selected and their mean, median, SD, and CV were determined (Table 1). Results indicated an average of 5.0% and 6.0% CV for Cy5 and Cy3 channels, respectively. Noises were negligible and did not correlate with PMT voltages; the deviations of measured intensities were within experimental errors ($<<10\%$). Repeated scanning up to 24 times did not decrease the fluorescence intensity, eliminating the concern of photo bleaching.

0022-1554/01/$3.30

Table 1 Repeated scanning of the same array 12 times at full laser power. Results for four different pixels in Cy5 and Cy3 channels indicated negligible photo bleaching and <<10% coefficients of variation

Pixel #	1		2		3		4	
Coordinate	X = 12390		X = 12600		X = 12790		X = 12980	
	Y = 9420		Y = 9420		Y = 9420		Y = 9630	
	Cy5	Cy3	Cy5	Cy3	Cy5	Cy3	Cy5	Cy3
50% PMT								
Mean	1027.4	3545.9	416.7	702.3	1966.3	2112.2	2215.5	1257.6
Median	1024.5	3534.5	409.5	708.5	1951.0	2103.0	2219.0	1261.0
SD	46.1	151.5	27.8	40.6	105.2	108.8	89.8	66.1
CV (%)	4.5	4.3	6.7	5.8	5.3	5.2	4.1	5.3
70% PMT								
Mean	13035.1	44865.2	5102.4	8514.1	25737.5	26482.1	29591.7	15903.5
Median	12969.5	45105.5	5135.5	8381.0	28009.5	28677.0	29519.5	15833.5
SD	537.4	2384.0	309.9	671.6	1550.0	2254.0	1514.2	554.9
CV (%)	4.1	5.4	6.1	7.9	6.1	8.5	5.1	3.5
75% PMT-Cy5, 70% PMT-Cy3								
Mean	19371.4	40990.5	7277.1	7487.8	36491.5	24824.8	41453.4	15200.2
Median	19359.5	41011.5	7366.0	7491.0	36285.5	25081.0	41727.0	15295.0
SD	511.8	2779.5	485.2	652.1	1310.1	1090.6	2236.6	954.6
CV (%)	2.6	8.8	8.7	8.7	3.6	4.4	5.4	6.3

Two properties regarding the RT-PCR amplification were examined: Do the amplified probes represent the true abundance of each transcript in cells? Does the probe saturate the arrays? First, we mixed five tk genes in three ratios (1, 20, and 400) and used them as PCR templates. Hybridizations of such PCR product to a small five-tk gene array showed a "compressed" ratio of three- to fourfold despite a 400-fold input template ratio. Nevertheless, the relative order of abundance of the five tk templates was conserved. Saturation has likely occurred in PCR, which may have also depleted some tk primers due to their high degeneracy. Second, we compared single-probe hybridizations at various concentrations. Four to six hundred ng of PCR amplified products typically were used for random prime labeling. The labeled probe was purified and different dilutions were applied to the arrays. It was determined that one tenth of the labeled probe per channel provided optimal signals for analysis without saturating the arrays.

Repeated hybridizations have identified distinctive patterns among thyroid, breast, and prostate cancer cell lines (Figure 1). Although the panel of 58 tk genes may not represent all the tk expressed in any single cancer

tissue, we have reason to believe they represent over 50% of human tk genes expressed in a particular tissue type (Robinson et al. 1996). These distinctive expression patterns, as unveiled by microarray, become molecular fingerprints of tk gene expression for each tumor.

Acknowledgments

Literature Cited

Celis JE, Kruhoffer M, Gromova I, Frederiksen C, Ostergaard M, Thykjaer T, Gromov P, Yu J, Palsdottir H, Magnusson N, Orntoft TF (2000) Gene expression profiling: monitoring transcription and translation products using DNA microarrays and proteomics. FEBS Lett 480:2–16

Cheung V, Morley M, Aguilar F, Massami A, Kucherlapati R, Childs G (1999) Making and reading microarrays. Nature Genet Suppl 21:15–19

DeRisi J, Penland L, Brown PO, Bittner ML, Meltzer PS, Ray M, Chen Y, Su YA, Trent JM (1996) Use of a cDNA microarray to analyze gene expression patterns in human cancer. Nature Genet 14:457–460

Iyer VR, Eisen MB, Ross DT, Schuler G, Moore T, Lee JC, Trent JM, Staudt LM, Hudson J, Boguski MS, Lashkari D, Shalon D, Botstein D, Brown PO (1999) The transcriptional program in the response of human fibroblasts to serum. Science 283:83–86

Robinson D, He F, Pretlow T, Kung HJ (1996) A tyrosine kinase profile of prostate carcinoma. Proc Natl Acad Sci USA 93:5958–5962

Schena M (1996) Genome analysis with gene expression microarrays. BioEssays 18:427–431

Figure 1 Multiple hybridizations confirmed distinctive patterns for three tumor cell lines. (**Array 1**) Prostate cancer cell lines Cy5:BPH-1-CAFTD-04/Cy3:BPH-1-CAFTD-02. (**Array 2**) Thyroid cancer cell lines Cy5:FTC133/Cy3:FTC236. (**Array 3**) Breast cancer cell line Cy5:MCF7/Cy3:58 tk mix.

Appendix 2

BRIEF REPORT

Monitoring Signal Transduction in Cancer: From Chips to FISH

Robert A. Lersch, Jingly Fung, H.-Ben Hsieh, Jan Smida, and Heinz-Ulrich G. Weier

Life Science Division, Lawrence Berkeley National Laboratory, Berkeley, California (RAL,H-BH,H-UGW); School of Medicine, University of California, San Francisco, California (JF); and Arbeitsgruppe Zytogenetik, gsf-Forschungszentrum für Umwelt und Gesundheit, Neuherberg, Germany (JS)

SUMMARY The microarray format of RNA transcript analysis should provide new clues to carcinogenic processes. Because of the complex and heterogeneous nature of most tumor samples, histochemical techniques, particularly RNA fluorescent in situ hybridization (FISH), are required to test the predictions from microarray expression experiments. Here we describe our approach to verify new microarray data by examining RNA expression levels of five to seven different transcripts in a very few cells via FISH. (J Histochem Cytochem 49:925–926, 2001)

KEY WORDS

spectral imaging

FISH

microarray

RNA

cancer

OUR LABORATORY is adapting microarray technology to identify new genes involved in the formation of tumors in the thyroid, breast, and prostate. Previously, the transcription levels of only a few genes could be assayed per experiment. Microarrays circumvent this limitation. However, a second problem limits progress in cancer research. Most tumors are a mix of cell types, due in part to the normal complexity of the tissue and in part to the complexity of tumors as they evolve from benign to metastatic. If researchers collect microarray data without confronting the problem of tumor heterogeneity, important correlations will be missed.

Preliminary studies performed in our lab and elsewhere indicated that solid tumors are heterogeneous with respect to oncogene expression. Figure 1 shows the expression of brk (O'Bryan et al. 1991) in a childhood thyroid cancer that arose after the Chernobyl nuclear accident (Zitzelsberger et al. 1999). In this case, two cells strongly express brk (arrows point to their nuclei) and a nearby cell does not express brk. These studies were performed with touchprep papillary thyroid tumor specimens using filter-based microscope systems and only two different cDNA probes. If

more than two probes are used per experiment, more slides, time, and reagents must also be used. All experiments involving human cells or cell lines were approved by the U.C. Berkeley Human Subject IRB.

To address this problem, we are developing a system to simultaneously measure cell-by-cell RNA levels of several different markers. The proposed scheme to discriminate benign and malignant neoplasms and to identify new prognostic markers will take advantage of new methods and our experience with oncogene activation in thyroid tumors. Our short-term goal is to develop a system which determines the relative level of expression of five tyrosine kinase genes using FISH-based methods and Spectral Imaging (SIm). Existing SIm instrumentation can record fluorescence spectra from 400 nm to 1100 nm with about 10-nm resolution, whereas the resolution of a light microscope is about 1 μm.

SIm combines the techniques of fluorescence microscopy, charge-coupled device (CCD) camera, and Fourier spectroscopy. The light emitted from each point of the sample is collected with the microscope objective and sent to a collimating lens. This light travels through an optical head (interferometer), is focused on a CCD camera, and the resulting data are processed with a computer. The interferometer divides each incoming beam (light from the microscope) into two coherent beams and creates a variable optical path difference (OPD) between them. The beams are then combined to interfere with each other. The resulting interference intensity is measured by the CCD detector as a function of the OPD. The intensity vs
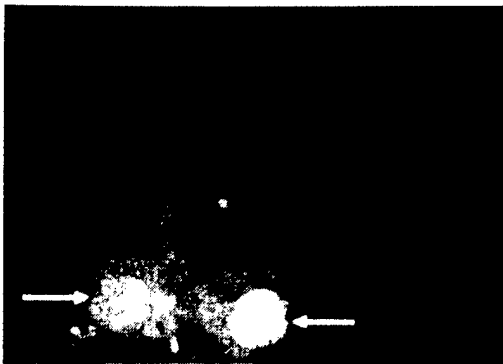
Figure 1 Frozen tissue touchprep of childhood thyroid tumor (S246) was hybridized with a cDNA probe for brk. The probe was labeled with digoxigenin and detected with rhodamine-conjugated antibodies. About 5% of the cells expressed brk at high levels, the other cells at low levels. Arrows indicate two high brk-expressing cells.

OPD is an "interferogram." The spectrum, i.e., intensity, as a function of wavelength can be recovered from the interferogram using Fourier transforms. The first published application of SIm (spectral karyotyping or SKY) (Schroeck et al. 1996) was developed to screen metaphase spreads for translocations with 24 chromosome-specific whole chromosome painting probes labeled with Spectrum Green, Spectrum Orange, Texas Red, Cy5, or Cy5.5, or combinations thereof. The multiple bandpass filter set (Chroma Technology; Brattleboro, VT) used for fluorochrome excitation was designed to provide broad emission bands (giving a fractional spectral reading from ~450 nm to ~850 nm).

Although we can use much of the existing technology, the ratio-labeling color scheme for SKY will not work for RNA detection because different labeled cDNA probes might co-localize. Therefore, we will label each cDNA probe with a unique reporter. The fluorescence spectra of the different reporter molecules can partially overlap, because the signals can be resolved by a computer algorithm termed "Spectral Un-Mixing (SUN)" (Applied Spectral Imaging; Carlsbad, CA). SUN enables us to deconvolute overlapping spectra and recover single component images from the spectral image.

The existing commercial SKY metaphase chromosome analysis software will be modified to increase its automated signal processing, RNA identification in interphase cells, integration of cDNA probe signals, and databasing of results. We will only refine the analysis software; the acquisition methods of capturing a spectral image and a separate high-contrast monochrome DAPI image will remain unchanged. A prototype of

this system for analysis of protein markers has already been developed (Tsurui et al. 2000) and will aid our efforts to analyze RNA transcript levels.

Initially we will hybridize cDNA probes to brk, ret, c-met, trk, axl/ufo (obtained from Research Genetics; Huntsville, AL) using five cyanine dyes (Amersham; Arlington Heights, IL). On the basis of previous microarray results, we will also add members of the Eph tyrosine kinase family. cDNA probes will be prepared by incorporating fluorochrome-labeled deoxynucleoside triphosphates by random priming or PCR amplification (Weier et al. 1994,1995). We will also build a reference spectra database for these probes. Standard fixation and hybridization protocols should detect the target RNAs. It is unclear if we will need to prepare custom blocking agents to DNA repeats in the 3'-untranslated region of some of our targets. Using artificial mixtures of existing cell lines, we will develop software modules needed to measure intracellular levels of five RNA species and to determine important process parameters: sensitivity, accuracy, and reproducibility.

Acknowledgments

Literature Cited

O'Bryan JP, Frye RA, Cogswell PC, Neubauer A, Kitch B, Prokop C, Espinosa R III, Le Beau MM, Earp HS, Liu ET (1991) axl, a transforming gene isolated from primary human myeloid leukemia cells, encodes a novel receptor tyrosine kinase. Mol Cell Biol 11:5016-5031

Schroeck E, du Manoir S, Veldman T, Schoell B, Wienberg J, Ferguson-Smith MA, Ning Y, Ledbetter DH, Bar-Am I, Soenksen D, Garini Y, Ried T (1996) Multicolor spectral karyotyping of human chromosomes. Science 273:494-497

Tsurui H, Nishimura H, Hattori S, Hirose S, Okumura K, Shirai T (2000) Seven-color fluorescence imaging of tissue samples based on Fourier spectroscopy and singular value decomposition. J Histochem Cytochem 48:653-662

Weier H-U, Polikoff D, Fawcett JJ, Greulich KM, Lee K-H, Cram S, Chapman VM, Gray JW (1994) Generation of five high complexity painting probe libraries from flow sorted mouse chromosomes. Genomics 24:641-644

Weier H-UG, Wang M, Mullikin JC, Zhu Y, Cheng J-F, Greulich KM, Bensimon A, Gray JW (1995) Quantitative DNA fiber mapping. Hum Mol Genet 4:1903-1910

Zitzelsberger H, Lehmann L, Hieber L, Weier H-UG, Janish C, Fung F, Negele T, Spelsberg F, Lengfelder E, Demidchik E, Salassidis K, Kellerer AM, Werner M, Bauchinger M (1999) Cytogenetic changes in radiation-induced tumors of the thyroid. Cancer Res 58:135-140

BRIEF REPORT

Monitoring Signal Transduction in Cancer: Tyrosine Kinase Gene Expression Profiling

Heinz-Ulrich G. Weier, Horst F. Zitzelsberger, H.-Ben Hsieh, Melita V. Sun, Mariwil Wong, Robert A. Lersch, Paul Yaswen, Jan Smida, Christine Kuschnick, and Orlo H. Clark

Life Sciences Division, University of California, E.O. Lawrence Berkeley National Laboratory, Berkeley, California (H-UGW, H-BH,MVS,RAL,PY); Arbeitsgruppe Zytogenetik, gsf-Forschungszentrum fuer Umwelt und Gesundheit, Neuherberg, Germany (HFZ,JS,CK); and Department of Surgery, University of California, San Francisco, California (MW,OHC)

SUMMARY Abnormal expression of tyrosine kinase (TK) genes is common in tumors, in which it is believed to alter cell growth and response to external stimuli such as growth factors and hormones. Although the etiology and pathogenesis of carcinomas of the thyroid or breast remain unclear, there is evidence that the expression of TK genes, such as receptor tyrosine kinases, or mitogen-activated protein kinases, is dysregulated in these tumors, and that overexpression of particular TK genes due to gene amplification, changes in gene regulation, or structural alterations leads to oncogenic transformation of epithelial cells. We developed a rapid scheme to measure semiquantitatively the expression levels of 50–100 TK genes. Our assay is based on RT-PCR with mixed based primers that anneal to conserved regions in the catalytic domain of TK genes to generate gene-specific fragments. PCR products are then labeled by random priming and hybridized to DNA microarrays carrying known TK gene targets. Inclusion of differently labeled fragments from reference or normal cells allows identification of TK genes that show altered expression levels during malignant transformation or tumor progression. Examples demonstrate how this innovative assay might help to define new markers for tumor progression and potential targets for disease intervention. (J Histochem Cytochem 49:673-674, 2001)

KEY WORDS
tyrosine kinase
tumors
RT-PCR
genes

BECAUSE the malignant transformation of epithelial cells and progression of carcinomas are accompanied by changes in the expression of receptor and cytosolic tyrosine kinase (TK) genes, we set out to develop an innovative DNA microarray-based assay to simultaneously determine the relative expression level of 50–100 TK genes using just a few cells.

A number of studies have shown that tumor development is accompanied by at least two changes: (a) a change in the way cells interact with their environment via membrane-bound receptors, and (b) a change in how

signals originating from these receptors are transduced from the cell membrane to the cytoplasm and the nucleus. Among the hundreds of genes involved in receptor-mediated signal transduction, only a few are aberrantly expressed in tumors. A major motif in signal transduction is the selective phosphorylation and dephosphorylation of tyrosine residues in protein factors involved in signal processing. Proteins that phosphorylate tyrosine residues are products of genes belonging to the family of TK genes. The number of known TK genes has grown steadily in recent years, and the temporal and tissue-specific expression of ~100 different TK genes in normal cells is carefully orchestrated. The level of expression of certain TK genes is increased in many human tumors (Luttrell et al. 1994; Liu et al. 1995). Simple overexpression of TK genes due to gene amplification or to changes in the regulation of gene expression may lead to oncogenic transformation. This has been clearly documented for the erbB2 protein, the product of the Her-2/neu proto-oncogene and other members of the erb B

family (Tse et al. 1997). In addition, many tumors have acquired structurally altered TK proteins or abnormal expression patterns through de novo mutational events. When chromosomes became rearranged, the catalytic domain of a TK gene was found fused to the amino terminal of another protein, thus creating a new transforming activity as well as a new expression pattern. Well-known examples of this mechanism of oncogene activation are the bcr/abl-fusion protein in chronic myeloid leukemia with a translocation, t(9;22), and the activation of the receptor TKs ret and trk in papillary thyroid cancer (Sozzi et al. 1992; Jhiang and Mazzaferri 1994).

Various protein factors can be mis-expressed and, in combination with other events, might constitute one of several factors leading to the onset and/or progression of cancer. Factors including cell cycle-specific enzymes, hormone receptors, and peptide growth factors have been reported as having prognostic significance in some cases of prostate cancer. Overexpression of particular receptor TK genes such as the insulin-like growth factor receptors (IGF-IRs), the epidermal growth factor receptor (EGFR or erb B) family of receptors, focal adhesion kinase (FAK), or the proto-oncogenes ret and Nyk/mer have been shown to correlate with progression to a more malignant phenotype in a variety of tumors (Resnik et al. 1998), among them carcinoma of the prostate (Ling and Kung 1995; Dawson et al. 1998). Detailed knowledge about TK gene expression and its relation to tumor progression might increase our understanding of how tumors grow and help us design assays to more accurately stage tumors.

Our project targets the development of a novel assay format that enables us to determine the level of expression of many different genes. A rapid assay uses DNA microarrays carrying small amounts of individual TK gene-specific targets to simultaneously determine the expression level of up to 100 TK genes using a small number of cells. We cloned and characterized TK genes expressed in thyroid cancers and in seven different breast cancer cell lines. Using mixed-base oligonucleotides specific for conserved domains in the catalytic domains of TK genes, our PCR assays amplified ~159–171-bp fragments of expressed TK genes. We size-selected and cloned the PCR products into plasmids. As of August 2000, we had identified more than 50 TK genes expressed in thyroid cancers plus an additional 172 TK fragment clones derived from breast cancer cell lines and ~250 TK fragment clones from radiation-induced thyroid cancers in the prescreening and sequencing steps. Previously, we finished the construction of a robotic system to print DNA microarrays with about 100 sequences on glass slides (unpublished data). The performance of the system was tested by hybridization of fluorochrome-labeled TK gene-specific PCR fragments onto the TK-specific DNA microarrays. All experiments involving human cells or

cell lines were approved by the U.C. Berkeley Human Subject Use Institutional Review Board. These experiments enabled us to optimize hybridization and washing conditions and to generate data regarding the relative level of gene expression. For example, the 184A1 and 184A1TH cell lines are closely related non-tumorigenic and tumorigenic human mammary epithelial cell lines derived from the same normal breast tissue specimen and transformed in vitro. After hybridizing Cy5-labeled TK fragments prepared from the cell line 184A1 and Cy3-labeled TK fragments prepared from cell line 184A1TH to a DNA microarray carrying 58 TK gene fragments and displaying Cy3 fluorescence signals in green and Cy5 signals in red, differences between the cell lines became readily apparent. Genes expressed at a higher level in 184A1TH cells led to increased green signals on the array, while those genes whose expression level is lower in 184A1TH cells compared to 184A1 cells generated spots that exhibited stronger red fluorescence. Similarly, differences between thyroid tumor cell lines could be demonstrated in simple dual-color hybridization experiments.

Acknowledgments

Literature Cited

Dawson DM, Lawrence EG, MacLennan GT, Amini SB, Kung HJ, Robinson D, Resnick I, Kursh ED, Pretlow TP, Pretlow TG (1998) Altered expression of RET proto-oncogene product in prostatic intraepithelial neoplasia and prostate. J Natl Cancer Inst 90:519–523

Jhiang SM, Mazzaferri EL (1994) The ret/PTC oncogene in papillary thyroid carcinoma. J Lab Clin Med 123:331–337

Ling L, Kung HJ (1995) Mitogenic signals, transforming potential of Nyk, a newly identified neural cell adhesion molecule-related receptor tyrosine kinase. Mol Cell Biol 15:6582–6592

Liu Y, el-Ashry D, Chen D, Ding IY, Kern FG (1995) MCF-7 breast cancer cells overexpressing transfected c-erbB-2 have an in vitro growth advantage in estrogen-depleted conditions, reduced estrogen-dependence, tamoxifen-sensitivity in vivo. Breast Cancer Res Treat 34:97–117

Luttrell DK, Lee A, Lansing TJ, Crosby RM, Jung KD, Willard D, Luther M, Rodriguez M, Berman J, Gilmer TM (1994) Involvement of pp60c-src with two major signaling pathways in human breast cancer. Proc Natl Acad Sci USA 91:83–87

Resnik JL, Reichart DB, Huey K, Webster NJ, Seely BL (1998) Elevated insulin-like growth factor I receptor autophosphorylation, kinase activity in human breast cancer. Cancer Res 58:1159–1164

Sozzi G, Bongarzone I, Miozzo M, Cariani CT, Mondellini P, Calderone C, Pilotti S, Pierotti MA, Della Porta G (1992) Cytogenetic, molecular genetic characterization of papillary thyroid carcinomas. Genes Chromosomes Cancer 5:212–218

Tse C, Brault D, Etienne J (1997) Current aspects of the evaluation of the ERBB2 activation in breast cancer. Therapeutic perspectives. Ann Biol Clin 55:545–554

Appendix 4

ELSEVIER

MCE

Towards a full karyotype screening of interphase cells: 'FISH and chip' technology

Heinz-Ulli G. Weier [a,*], Santiago Munné [b], Robert A. Lersch [a], H.-Ben Hsieh [a], Jan Smida [c], Xiao-Ning Chen [d], Julie R. Korenberg [d], Roger A. Pedersen [e], Jingly Fung [a,e]

[a] *Department of Subcellular Structure, Life Sciences Division MS 74-157, University of California, E.O. Lawrence Berkeley National Laboratory, 1 Cyclotron Road, Berkeley, CA 94720, USA*
[b] *The Institute for Reproductive Medicine and Science, Saint Barnabas Medical Center, Livingston, NJ 07052, USA*
[c] *Institute of Radiobiology, GSF-Forschungszentrum für Umwelt und Gesundheit GmbH, D 85758 Oberschleissheim, Germany*
[d] *Medical Genetics Birth Defects Center, University of California, Los Angeles, CA 90048, USA*
[e] *Department of Obstetrics, Reproductive Genetics Unit, Gynecology and Reproductive Sciences, University of California, San Francisco, CA 94143-0720, USA*

Abstract

Numerical chromosome aberrations are incompatible with normal human development. Our laboratories develop hybridization-based screening tools that generate a maximum of cytogenetic information for each polar body or blastomere analyzed. The methods are developed considering that the abnormality might require preparation of case-specific probes and that only one or two cells will be available for diagnosis, most of which might be in the interphase stage. Furthermore, assay efficiencies have to be high, since there is typically not enough time to repeat an experiment or reconfirm a result prior to fertilization or embryo transfer. Structural alterations are delineated with breakpoint-spanning probes. When screening for numerical abnormalities, we apply a Spectral Imaging-based approach to simultaneously score as many as ten different chromosome types in individual interphase cells. Finally, DNA micro-arrays are under development to score all of the human chromosomes in a single experiment and to increase the resolution with which micro-deletions can be delineated. © 2001 Elsevier Science Ireland Ltd. All rights reserved.

Keywords: Cytogenetics; Chromosomes; Hybridization; FISH; DNA micro-arrays; Digital image analysis (blastomeres)

1. Introduction

Carriers of balanced translocations have an elevated risk of producing aneuploid germ cells due to disturbed homologue pairing. The resulting partial or total aneusomies lead to spontaneous abortions, stillbirth or severe deficiencies and disease. Assisted reproductive technology now offers couples at risk several diagnostic approaches to reduce the risk of carrying an affected fetus. If the woman carries the abnormality, first polar bodies can be analyzed immediately after oocyte harvest. Following in vitro fertilization, pre-implantation genetic analysis (PGD) can be performed on individual blastomeres biopsied from 3-day-old embryos. Since most of the embryonic cells will be found in interphase stage, the diagnostic approach will have to work reliably with either the less condensed chromatin in interphase cell nuclei or the highly condensed DNA in polar bodies (PB's).

Our collaborating laboratories have long been involved in the development of nucleic acid hybridization-based procedures for the rapid detection of structural and numerical chromosome abnormalities. Here, we report the present state of hybridization-based technologies for interphase cell analysis in PGD. Since only one or two cells are available for analysis, our approaches are geared towards obtaining a maximum of cytogenetic information per experiment.

* Corresponding author. Tel.: + 1-510-486-5347; fax: + 1-510-486-5343.
E-mail address: ugweier@lbl.gov (H.-U.G. Weier).

2. Material and methods

For more than a decade, our laboratories have been involved in the development of technologies for analysis of interphase and metaphase cells. In collaboration with scientists at the University of California, San Francisco, and the St Barnabas Medical Center, Livingston, researchers at the E.O. Lawrence Berkeley National Laboratory study the chromosomal composition of blastomeres with regard to numerical as well as structural aberrations. The technical aspects of our probe preparation and multicolor detection protocols have been published previously (Weier et al., 1994; Jossart et al., 1996; Cassel et al., 1997).

A major goal of our technical developments is to maximize the number of chromosomal targets that can be scored simultaneously. Briefly, probes specific for repeated DNA on chromosomes 15, X, and Y purchased from Vysis (Downers Grove, IL) were labeled with either a green or red fluorochrome (Spectrum Green or Spectrum Orange, respectively). The probes specific for chromosome 9, 13, 14, 16, 18, 21, and 22 were prepared in house and labeled by random priming (BioPrime Kit, GIBCO/LTI, Gaithersburg, MD) incorporating biotin-14-dCTP (part of the BioPrime Kit), digoxigenin-11-dUTP (Roche Molecular Biochemicals, Indianapolis, IN), fluorescein-12-dUTP (Roche Molecular Biochemicals) (Weier et al., 1995), or Cy3-dUTP (Amersham, Arlington Heights, IN). Bound biotinylated probes were detected with avidin-Cy5, and bound digoxigenin-labeled probes were detected with Cy5.5-conjugated antibodies against digoxin (Sigma, St. Louis, MO). Between 0.5 and 3 µl of each probe along with 1 µl human COT1™ DNA (1 mg/ml, GIBCO/LTI) and 1 µl salmon sperm DNA (20 mg/ml, 3′–5′, Boulder, CO) were precipitated with 1 µl glycogen (Roche Molecular Biochemicals, 1 mg/ml) and 1/10 volume of 3 M sodium acetate in 2 volumes of 2-propanol, air dried and resuspended in 3 µl water, before 7 µl of hybridization master mix [78.6% formamide (FA, GIBCO/LTI), 14.3% dextran sulfate in 2.9 × SSC, pH 7.0 (1 × SSC is 150 mM NaCl, 15 mM Na citrate)] were added. This gave a total hybridization mixture of 10 µl.

All blastomeres used in the probe developments were obtained from embryos donated by patients enrolled in the IVF Programs of The University of California, San Francisco, or The Institute for Reproductive Medicine and Science of Saint Barnabas Medical Center. In accordance with guidelines set by the internal review boards of these Medical Centers, written consent was obtained from the patients in each case. Embryo biopsies and blastomere fixations were carried out as described (Munné et al., 1994, 1996). As indicated below, embryos used for some studies had arrested development or were morphologically abnormal.

3. Results and discussion

Traditional filter based microscope systems limited fluorescence in situ hybridization (FISH) experiments to the simultaneous use of typically no more than three to five differently labeled probes for interphase analysis (Munné and Weier, 1996). This is sufficient to detect structural alterations in interphase and metaphase cells or score a few chromosomes in interphase cells (Munné et al., 1994; Munné and Weier, 1996; Munné et al., 1996). We prepared case-specific breakpoint-spanning probe contigs to identify intrachromosomal rearrangements such as inversions or deletions (Cassel et al., 1997). The same approach can be used to demonstrate interchromosomal rearrangements such as reciprocal translocations (Munné et al., 1998a; Fung et al., 1999; Weier et al., 1999). The case-specific probes allow one to discriminate between a normal karyotype, aneuploid cells, and a balanced karyotype carrying the derivative chromosomes. A less time consuming and, thus, less expensive approach using DNA probes that bind distal to the respective breakpoints can only be used to count the number of chromosome copies and thus cannot discriminate between the normal and the balanced karyotypes (Munné et al., 1998b).

3.1. Detection of structural chromosome aberrations

Our scheme for the detection of structural alteration is based on the preparation and hybridization of two differently labeled DNA probes that bind on both sides of the respective chromosome breakpoints (Cassel et al., 1997). One probe will be detected in the green fluorescence wavelength interval, while the second probe is made such that it fluoresces red. Normal homologues lack the rearrangement and the probes produce large hybridization domains that appear either red or green in the fluorescence microscope. At the same time, we counterstain the DNA with 4,6-diamino-2-phenylindole (DAPI) which fluoresces blue under ultraviolet light excitation. If the cell contains a derivative chromosome, the hybridization result will show a red/green associated or partially overlapping signal indicative of the translocation event. Thus, we detect structural alteration and score homologues at the same time.

Our work is greatly facilitated by access to resources created in the course of the International Human Genome Sequencing Project, such as large insert genomic DNA libraries (bacterial or yeast artificial chromosomes (BACs or YACs, respectively), high resolution physical maps or collections of cytogenetically mapped DNA probes (Chen et al., 1996; Kim et al., 1996; Korenberg et al., 1999). This enables us to prepare case-specific probe sets suitable for interphase cell analyses of most patient cells within a few weeks.

Once optimized, these probe sets allow to rapidly determine the exact number of normal chromosomes and derivative chromosomes in somatic cells from translocation carriers as well as their germ cells or offspring. So far, however, these procedures failed to produce the desired increase in pregnancy rates in cases where one spouse carried a balanced reciprocal translocation. Our concern is that the impaired homologue pairing in the carriers leads to gain or loss of other chromosomes which remains undetected in assays scoring only the translocation chromosomes.

The recent introduction of Spectral Imaging (SIm) now allows one to interrogate a much larger number of targets, thus producing a more comprehensive picture of the chromosomal composition of the cells. SIm allows an investigator to discriminate an increased number of fluorescent probes by exciting fluorescent molecules over a broad spectral range and by recording the fluorescence emission spectral using an interferometer.

3.2. Detection of numerical chromosome abnormalities using Spectral Imaging (SIm)

Chromosome abnormalities occur with astonishing frequency in humans, being present in an estimated 10–30% of all fertilized eggs. Over 25% of all the miscarriages are monosomic or trisomics, making aneuploidy the leading known cause of pregnancy loss. Ideally, one likes to detect aneuploidy involving any of the 24 human chromosomes for preimplantation genetic and prenatal diagnosis. Thus, an analytical method to enumerate as many chromosomes as possible in few interphase cells is highly desirable. Using a set comprized of seven chromosome-specific probes (chromosome 10, 14, 16, 18, 22, X and Y) hybridized to lymphocyte interphase nuclei, we demonstrated that Spectral Imaging system provides a significant improvement over conventional filter-base microscope systems for enumeration of multiple chromosomes in interphase nuclei (Fung et al., 1998b).

Using mostly yeast or bacterial artificial chromosome probes for cytogenetic analyses of blastomeres and detection of structural alterations, we are building panels of probes to simultaneously score 10 or more different chromosomes. Further increases in the number of probes is complicated due to occasional overlap of chromosome domains or local variation in hybridization efficiency. We developed a 10-chromosomes probe set (chromosomes 9, 13, 14, 15, 16, 18, 21, 22, X and Y) for the purpose of labeling DNA targets most frequently associated with aneuploidy and spontaneous abortions and tested its application in PGD (blastomeres from abnormal human preimplantation embryos) and prenatal diagnosis (uncultured amniocytes obtained by amniocentesis). Results demonstrated in-

creasing levels of background fluorescence on different cells after hybridization in the order: (uncultured amniocytes) >> (blastomeres) > (interphase cells from lymphocytes). All blastomeres fixed for this study ($N = 25$) spread very well. Fourteen nuclei (56%) showed interpretable hybridization results, and most of them were karyotyped as abnormal, since all those cells were from 1 and 3 PN human embryos, and had arrested development or were morphologically abnormal. The signals from 11 nuclei (44%) were faint. This may be related to the quality of the embryos, since all of them were developing abnormally. The fixation of uncultured amniocytes on slides for Spectral Imaging analysis turned out to be somewhat difficult. Most nuclei were not flattened out, presenting a problem due to the limited focal depth. Overlapping signal domains were a problem in uncultured amniocytes, where only about 20% of all cells showed interpretable spreads. In summary, Spectral Imaging has demonstrated advantages for evaluating numerical chromosomal abnormalies in single interphase cells. Its utility for chromosome scoring, however, remains limited due to chromosome domain overlap.

3.3. DNA micro-arrays (chips)

The DNA micro-arrays represent an exciting new technology with applications ranging from gene expression profiling to determination of gene copy number changes in tumors. We are presently investigating this approach in which the DNA probes are immobilized on glass slides as a strategy complementing FISH studies. The DNA from the embryonic cells is labeled in one color (e.g. red), while an equal amount of a reference DNA probe is labeled in a different color (e.g. green). These differentially labeled DNA are combined, denatured and hybridized to a DNA micro-array or 'chip' in a quantitative manner. Results are obtained after reading the micro-arrays with specially designed fluorescence scanners as red/green or red/infrared fluorescence ratios. After normalization, every increase or decrease from the average ratio indicates an abnormal number of copies of the hybridization target.

In practice, the DNA contained in a single cell is not sufficient to generate measurable signals. The commonly used protocols therefore include a DNA in vitro amplification step using a random primer or oligonucleotide with arbitrary sequence prior to labelling. The DNA to be immobilized can be obtained by standard isolation protocols or by in vitro DNA amplification. We use a DNA spotter based on the design published by Brown's group at Stanford University (Schena et al., 1996). This allows us to spot small amounts of DNA on poly-L-lysine coated glass slides with a 100–200 micron pitch. A 288-spot DNA micro-array like the test array depicted schematically in Fig. 1 then measures no more
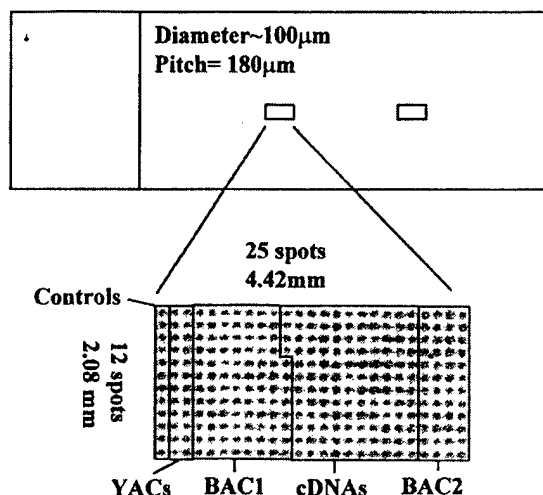
Fig. 1. Prototype DNA micro-array for technology development. The chip contains from left to right: control DNA spots (six samples), PCR amplified YAC DNA (12 clones), BAC array 1 (46 clones for copy number determination in breast cancer research), cDNA (62 tyrosine kinase cDNA for expression profiling), and BAC array 2 (24 clones for chromosome enumeration in PGD). All samples are spotted in duplicate. The total number of DNA spots of 300 arrayed with a 180 μm pitch leads to array dimensions of 2.08 × 4.42 mm^2. Each slide contains two identical micro-arrays.

than a few square millimeters. This small size of micro-arrays is an advantage over larger arrays prepared on nylon filters, because it requires less amount of labeled DNA sample in the hybridization reaction.

We are presently preparing DNA test chips to develop the methods and study parameters such as probe preparation, hybridization conditions and chip reader performance. Our long term objective is the development of reliable procedures to detect structural as well as numerical abnormalities using a combination of 'FISH and chip' technology. Chips to be used in those studies will carry several hybridization targets per chromosome arm, thus allowing a more detailed gene dosage determination or delineation of full or partial aneusomies than the FISH-based assays.

References

Cassel, M.J., Munné, S., Fung, J., Weier, H.U.G., 1997. Carrier-specific breakpoint-spanning DNA probes: an approach to pre-implantation genetic diagnosis [PGD] in interphase cells. Hum. Reprod. 12, 101–109.

Chen, X.-N., Mitchell, S., Sun, Z.G., Noya, D., Ma, S., Sekhon, G.S., Thompson, K., Hsu, W.-T., Wong, P., Wang, N., Shcreck, R., Falk, R., Korenberg, J.R., 1996. The Integrated BAC Resource: a powerful new molecular tool for prenatal genetics. Am. J. Hum. Genet. 59, A12.

Fung, J., Munné, S., Duell, T., Weier, H.-U.G., 1998a. Rapid cloning of translocation breakpoints: from blood to YAC in 50 days. J. Biochem. Mol. Biol. Biophys. 1, 181–192.

Fung, J., Hyun, W., Dandekar, P., Pedersen, R.A., Weier, H.-U.G., 1998b. Spectral imaging in preconception/preimplantation genetic diagnosis (PGD) of aneuploidy: multi-colour, multi-chromosome screening of single cells. J. Ass. Reprod. Genet. 15, 322–329.

Fung, J., Munné, J., Garcia, J., Kim, U.-J., Weier, H.-U.G., 1999. Reciprocal translocations and infertility: molecular cloning of breakpoints in a case of constitutional translocation t(11;22)(q23;q11) and preparation of probes for preimplantation genetic diagnosis (PGD). Reprod. Fert. Devel. 11, 17–23.

Jossart, G.H., O'Brien, B., Cheng, J.-F., Tong, Q., Jhiang, S.M., Duh, Q., Clark, O.H., Weier, H.-U.G., 1996. A novel multicolor hybridization scheme applied to localization of a transcribed sequence (D10S170/H4) and deletion mapping in the thyroid cancer cell line TPC-1. Cytogenet. Cell Genet. 75, 254–257.

Kim, U.J., Shizuya, H., Kang, H.L., Choi, S.S., Garrett, C.L., Smink, L.J., Birren, B.W., Korenberg, J.R., Dunham, I., Simon, M.I., 1996. A bacterial artificial chromosome-based framework contig map of human chromosome 22q. Proc. Natl. Acad. Sci. USA 93, 6297–6300.

Korenberg, J.R., Chen, X.-N., Sun, Z., Shi, Z.-Y., Shi, Ma.S., Vataru, E., Yimlamai, D., Weissenbach, J.S., Shizuya, H., Melvin, S.I., Gerety, S.S., Nguyen, H., Zemsteva, I.S., Hui, L., Silva, J., Wu, X., Birren, B.W., Hudson, T.J., 1999. Human Genome Anatomy: BACs integrating the genetic and cytogenetic maps for bridging genome and biomedicine. Genome Res. 9, 994–1001.

Munné, S., Grifo, J., Cohen, J., Weier, H.-U.G., 1994. Mosaicism and aneuploidy in arrested human preimplantation embryos: a multiple probe fluorescence in situ hybridization (FISH) study. Am. J. Hum. Genet. 55, 150–159.

Munné, S., Dailey, T., Finkelstein, M., Weier, H.U.G., 1996. Reduction in overlaps and missing signals in interphase-FISH. J. Assist. Reprod. Genet. 13, 149–156.

Munné, S., Weier, H.-U.G., 1996. Simultaneous enumeration of chromosomes X, Y, 18, 13, and 21 in interphase cells for preimplantation genetic diagnosis of aneuploidy. Cytogenet. Cell Genet. 75, 264–270.

Munné, S., Fung, J., Cassel, M.J., Márquez, C., Weier, H.-U.G., 1998a. Preimplantation genetic analysis of translocations: case-specific probes for interphase cell analysis. Hum. Genet. 102, 663–674.

Munné, S., Morrison, L., Fung, J., Márquez, C., Weier, U., Bahçe, M., Sable, D., Grundfelt, L., Schoolcraft, B., Scott, R., Cohen, J.,

1998b. Spontaneous abortions are significantly reduced after pre-conception genetic diagnosis of translocations. J. Ass. Reprod. Genet. 15, 290–296.

Schena, M., Shalon, D., Heller, R., Chai, A., Brown, P.O., Davis, R.W., 1996. Parallel human genome analysis: microarray-based expression monitoring of 1000 genes. Proc. Natl. Acad. Sci. USA 93, 10614–10619.

Weier, H.-U., Rosette, C.D., Matsuta, M., Zitzelsberger, H., Matsuta, M., Gray, J., 1994. Generation of highly specific DNA hybridization probes for chromosome enumeration in human interphase cell nuclei: isolation and enzymatic synthesis of alpha satellite DNA probes for chromosome 10 by primer directed DNA amplification. Meth. Mol. Cell Biol. 4, 231–248.

Weier, H.-U.G., Wang, M., Mullikin, J.C., Zhu, Y., Cheng, J.F., Greulich, K.M., Bensimon, A., Gray, J.W., 1995. Quantitative DNA fiber mapping. Hum. Mol. Genet. 4, 1903–1910.

Weier, H.-U.G.; Munné, S., Fung, J., 1999. Patient-specific probes for preimplantation genetic diagnosis (PGD) of structural and numerical aberrations in interphase cells. J. Assist. Reprod. Genet. 16, 182–189.

Appendix 5

UICC   Publication of the International Union Against Cancer

Clonal Chromosomal Aberrations in Simian Virus 40-Transfected Human Thyroid Cells and in Derived Tumors Developed after In Vitro Irradiation

Horst Zitzelsberger, Ph.D.,[1,2]* Jochen Bruch, Ph.D.,[1] Jan Smida, Ph.D.,[1]
Ludwig Hieber, Ph.D.,[1] Clare M. Peddie, Ph.D.,[3] Peter E. Bryant, Ph.D.,[3]
Andrew C. Riches, Ph.D.,[3] Jingly Fung, Ph.D.,[4] Heinz-Ulrich G. Weier, Ph.D.,[5]
and Manfred Bauchinger, Ph.D.,[1]

[1]*Institute of Radiobiology, GSF-Forschungszentrum für Umwelt und Gesundheit GmbH, Neuherberg, Germany*
[2]*Institute of Radiation Biology, Ludwig Maximilians University, Munich, Germany*
[3]*School of Biology, University of St. Andrews, St. Andrews, Fife, Scotland*
[4]*Reproductive Sciences Group, Department of Obstetrics/Gynecology, University of California, San Francisco, California*
[5]*Life Sciences Division, E.O. Lawrence Berkeley National Laboratory, Berkeley, California*

SUMMARY In vitro model cell systems are important tools for studying mechanisms of radiation-induced neoplastic transformation of human epithelial cells. In our study, the human thyroid epithelial cell line HTori-3 was analyzed cytogenetically following exposure to different doses of α- and γ-irradiation and subsequent tumor formation in athymic nude mice. Combining results from G-banding, comparative genomic hybridization, and spectral karyotyping, chromosome abnormalities could be depicted in the parental line HTori-3 and in nine different HTori lines established from the developed tumors. A number of chromosomal aberrations were found to be characteristic for simian virus 40 immortalization and/or radiation-induced transformation of human thyroid epithelial cells. Common chromosomal changes in cell lines originating from different irradiation experiments were loss of 8q23 and 13cen-q21 as well as gain of 1q32-qter and 2q11.2-q14.1. By comparison of chromosomal aberrations in cell lines exhibiting a different tumorigenic behavior, cytogenetic markers important for the tumorigenic process were studied. It appeared that deletions on chromosomes 9q32-q34 and 7q21-q31 as well as an increased copy number of chromosome 20 were important for the tumorigenic phenotype. A comparative breakpoint analysis of the marker chromosomes found and those observed in radiation-induced childhood thyroid tumors from Belarus revealed a coincidence for a number of chromosome bands. Thus, the data support the usefulness of the established cell system as an in vitro model to study important steps during radiation-induced malignant transformation in human thyroid cells.   © 2001 Wiley-Liss, Inc.

INTRODUCTION

The neoplastic transformation of normal human ep-
ithelial cells to cancer cells is a multistep process
associated with immortalization. aberrant growth
control. and malignancy [1]. For a detailed under-
standing of this multistage nature of human carci-
nogenesis, it is essential to develop in vitro models
of human epithelial cell transformation. So far, a
number of human epithelial cell lines from skin.
bronchus. thyroid gland, prostate. and ureteral tis-
sue have been immortalized using viral constructs.
In four of these cell lines [1–7]. tumor formation in
athymic nude mice was observed following irradia-
tion in vitro. For the immortalization process. viral
vectors (simian virus 40 [SV40]. Epstein Barr. ad-
enovirus. and human papillomavirus) have been
used that function through the dysregulation of the
p53 gene and DNA damage-induced checkpoints.
Cell lines immortalized in this way are often ge-
netically unstable and exhibit complex rearranged
karyotypes complicating the identification of cyto-
genetic markers related to radiocarcinogenesis.
G-banding analysis is not sufficient to resolve com-
plex changes and also to detect hidden abnormali-
ties so, therefore. molecular cytogenetic techniques
such as spectral karyotyping (SKY) and compara-
tive genomic hybridization (CGH) must be addi-
tionally applied. SKY has been developed to char-
acterize human metaphase spreads after
simultaneously hybridizing the chromosomes with
24 chromosome-specific whole chromosome paint-
ing probes [8]. This combination of spectroscopic
detection methods and in situ hybridization assays
using fluorescently tagged probes allows a simul-
taneous depiction and analysis of the whole human
chromosome complement. Interchromosomal rear-
rangements can be recognized as differentially
stained chromosome segments. thus greatly facili-
tating the characterization of structural aberrations,
especially those with complex patterns [8–10] and
of hidden chromosome abnormalities [11,12]. If
this technique is used in addition to comparative
genomic hybridization [13], which depicts copy
number changes with high accuracy, a comprehen-
sive picture of chromosomal abnormalities devel-
oped during the neoplastic cell transformation can
be obtained.

In our study, SV40-immortalized and radia-
tion-transformed human thyroid cell lines (HTori)
were analyzed cytogenetically by G-banding. SKY

and CGH. We investigated the immortalized paren-
tal cell line as well as nine radiation-transformed
(α- and γ-irradiated with different doses) cell lines
and identified specific chromosomal changes at-
tributable to the immortalization process. the tu-
morigenic behavior. and/or the different radiation
qualities.

MATERIALS AND METHODS

Cell Cultures

The human thyroid epithelial cell line (HTori-3)
used in our study was originally derived by trans-
fecting the epithelial cells with a plasmid contain-
ing the origin of replication defective SV40 ge-
nome [14]. The cells were cultured in medium
consisting of equal volumes of Dulbecco's modi-
fied Eagle's medium and Ham's F12 medium
supplemented with 7% fetal calf serum. penicillin
(10 units per ml). streptomycin (100 μg per ml) and
L-glutamine (2 mM). It has previously been dem-
onstrated that following irradiation of these cells in
vitro with either single doses of gamma irradiation
or alpha particle irradiation that tumors developed
in athymic nude mice following transplantation of
the irradiated cells [4,6,7]. Cells were not pooled at
any stage so that the resulting tumors must be re-
garded as independent events. The unirradiated
cells in these series of experiments did not produce
tumors in athymic nude mice. Cell lines were de-
rived from the primary tumors. Three of these tu-
mor cell lines will be utilised in this study. The first
line (HTG1) was derived from cells exposed to
0.5 Gy gamma irradiation. A tumor was detected
17 weeks after injection into athymic nude mice
and was removed at 25 weeks when the tumor was
8 mm in diameter. A further two tumor cell lines
(HTA3 and HTA6) were derived from cells ex-
posed to 0.25 Gy and 0.5 Gy alpha particle irradia-
tion. The tumor HTA3 was detected at 13 weeks
after injection and was removed at 17 weeks when
the tumor diameter was 8 mm. Similarly HTA6 was
detected at 17 weeks and removed at 23 weeks
when two tumors of 6 mm in diameter were pres-
nt. Following establishment of cell lines in vitro
from the primary tumors, cloned cell lines were
derived. From the HTG1 primary cell line, two
lines were derived (HTG1cl1 and HTG1cl3). Simi-
larly cloned cell lines were derived from the HTA3
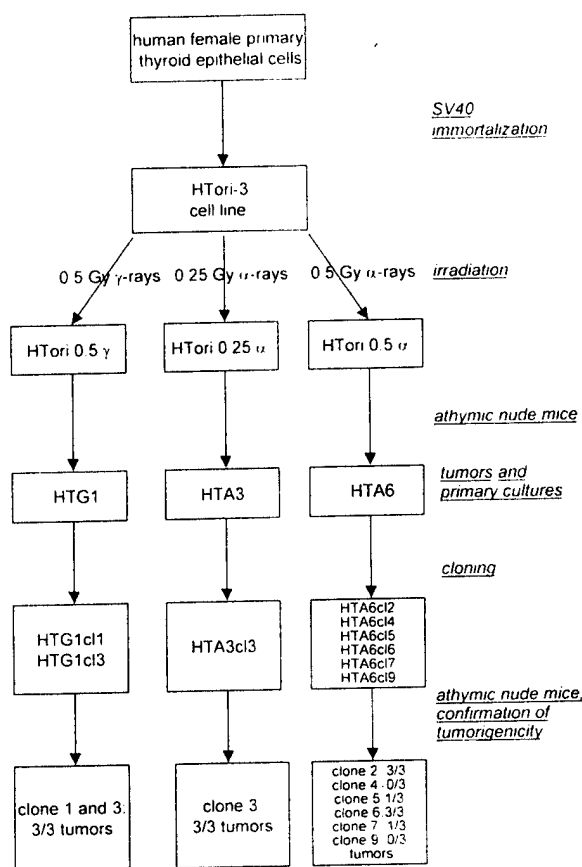primary cell line (HTA3cl3) and the HTA6 primary

Fig. 1. HTori cell lines established from primary thyroid epithelial cells following SV40 immortalization and radiation-induced transformation. Cell lines had been tested for tumorigenicity in athymic nude mice. Cultures were established from the primary tumors that developed and cell lines generated from cloned cells.

cell line (HTA6cl2, HTA6cl4, HTA6cl5, HTA6cl6, HTA6cl7 and HTA6cl9). The origins of the cell lines are summarised in Figure 1.

Tumorigenicity Screening

The cloned cell lines derived from primary tumor cell lines HTG1 (two lines), HTA3 (one line) and HTA6 (six lines) were screened for tumorigenicity in athymic nude mice. Cells (2–3 × 10⁶) were injected subcutaneously into the dorsal region of three athymic nude mice. The mice were screened for tumor development for 5 months and scored positively if tumors of greater than 3 mm diameter growing progressively were detected.

G-Banding

Cells were seeded onto glass slides and metaphase spreads were prepared after in vitro culture of cells for several days following standard procedures. After G-banding with Wright's staining solution,

karyotyping was performed according to the International System for Human Cytogenetic Nomenclature (ISCN) [15].

Spectral Karyotyping

SKY analysis was performed as described previously [10]. Briefly, chromosome preparations were aged for two weeks at room temperature. Metaphase spreads were pretreated with RNase A (0.1 mg/ml in 2 × SSC) and pepsin solution (10 µg/ml in 0.01 M HCl) and fixed in 1% formaldehyde. Pepsin digestion was performed under microscopic control. Slides were placed in denaturing solution (70% formamide [FA] in 2 × SSC) at 70°C for 150 sec and dehydrated in a 70%, 80%, 100% ethanol series. Subsequently, spreads were hybridized with a probe mixture supplied by Applied Spectral Imaging (ASI, Carlsbad, Calif.). The probe mixture contained 24 whole chromosome painting probes, labeled with combinations of five different fluorescent dyes (Spectrum Green, Spectrum Orange, Texas Red, Cyanine [Cy] 5 and Cy5.5) [16]. The probe (SKY™ mixture) was denatured at 75°C for 7 min and incubated at 37°C for 1 hr. The hybridization solution was applied to the denatured metaphases and incubated for two days at 37°C. Posthybridization washes were performed in 50% FA/2 × SSC (three times for 5 min) at 45°C, 1 × SSC (twice for 5 min) and in 4 × SSC/0.1% Tween 20, (2 min at 20°C). Detection of biotinylated probes was performed with avidin-Cy5. Digoxigenin-labeled probes were detected with a mouse anti-digoxigenin antibody followed by a goat anti-mouse antibody conjugated to Cy5.5. Metaphase spreads were stained with 4′,6-diamidino-2-phenylindole (DAPI) solution (150 ng/ml in 2 × SSC) and covered with antifade solution (Vectashield mounting medium; Vector Laboratories, Burlingame, Calif.). Metaphase images were acquired by use of a SpectraCube system (ASI) and analyzed with the SKYView imaging software [17]. Aberrations were described according to the ISCN nomenclature [15].

Comparative Genomic Hybridization (CGH)

CGH was performed on cell lines as described [18,19] with slight modifications. Briefly, whole genomic DNA was isolated from the cell lines according to standard procedures and labeled with biotin-16-dUTP (Roche Molecular Biochemicals, Mannheim, Germany) and biotin-11-dCTP (Life Technologies, Eggenstein, Germany) by nick-translation. Normal female reference DNA was isolated from peripheral lymphocytes of a healthy

donor and labeled with cy3-conjugated dUTP and dCTP (Amersham, Braunschweig, Germany). After hybridization to normal metaphase spreads of a healthy male donor, the biotin-labeled DNA was detected with avidin-FITC (Vector Laboratories) (diluted in 0.1 M sodium phosphate, pH 8.0, 0.1% nonidet-P40, 0.1% sodium azide plus 5% nonfat dry milk). After washes in PN buffer (0.1 M sodium phosphate, pH 8.0, 0.1% nonidet-P40), slides were counterstained with DAPI (150 ng/ml in 2×SSC) for karyotyping and mounted in antifade solution. For CGH analysis, at least 10 metaphases were imaged and karyotyped using a Zeiss Axioplan 2 fluorescence microscope equipped with filter sets (single-band excitation filters) for DAPI, fluorescein, and tetramethylrhodamine isothiocyanate (TRITC). Averaged profiles were generated by a CGH analysis software (MetaSystems, Altlussheim, Germany) from at least 10 to 15 homologous chromosomes and interpreted according to published criteria [18,20].

RESULTS

Ten HTori cell lines were investigated cytogenetically by G-banding, SKY, and CGH, among them the parental cell line HTori-3 as well as nine radiation-induced tumor cell lines (Fig. 1). The results of the tumorigenicity screening of the nine cloned cell lines are summarised in Figure 1. Most of the cloned lines were tumorigenic in athymic nude mice. Two of the cloned lines (HTA6cl4 and HTA6cl9) derived from the HTA6 primary cell line failed to produce tumors.

G-banding analysis revealed a near-pentaploid chromosome number in cell line HTA3cl3, while all other cell lines appeared to have a hypotriploid chromosome number and various marker chromosomes that could not be classified further.

Therefore, a detailed cytogenetic characterization was only feasible combining results from SKY and CGH analysis. For SKY analysis, about 4 to 10 metaphases were analyzed from each cell line. A total of 79 clonal markers (M1 to M79), i.e., structurally rearranged or deleted chromosomes appearing in at least two metaphases, were identified (Table 1). Some of the markers have very similar breakpoints (M1/M2, M9/M11, M20/M21, M23/M24, M44/M47, M58/M59/M60, M69/M70) and differ only in one translocation partner chromosome.

Twenty-three different immortalization markers were identified by SKY analysis of the parental cell line. They are indicated in Tables 1 and 2 with a single underline and examples of some of these markers are shown in Figure 2. Additional changes

in the immortalized HTori-3 cell line are gains on 4p, 5q, 6p, 16p, 17q, 20, 21, and 22 as well as losses on 3p, 11q, 18q, and X (Table 3). Cytogenetic markers that appeared exclusively in cell lines originating from γ-ray-induced tumors (HTG1cl1, HTG1cl3) or in cell lines developed from α-ray-induced tumors (HTA3cl3 and HTA6 clones) are marked in Table 2 by dotted and double underlines, respectively. In cell lines originating from γ-ray-induced tumors, markers M16, M26, M27, M30, M35, M39, M41, and M52 became apparent, whereas markers M6, M8, M15, M17, M18, M21, M34, M69, and M72 were detected exclusively in cell lines developed from α-ray-induced tumors (Fig. 3).

Cytogenetic markers obviously related to the tumorigenic process were studied in HTA6 clones showing a different tumorigenic behavior. Clones HTA6cl2 and HTA6cl6 induced the same tumor frequency as the corresponding primary culture, whereas HTA6cl5 and HTA6cl7 showed a reduced and HTA6cl4 and HTA6cl9 a completely missing tumorigenic behavior in nude mice. In the tumorigenic lines HTA6cl2, HTA6cl6, HTG1cl1, and HTG1cl3, loss of 9q32-q34 became apparent. Additionally, loss of 7q21-q31 and an increased copy number of chromosome 20 (four copies) appeared to be indicative for tumorigenic lines. The nontumorigenic cell line HTA6cl9 as well as lines HTA6cl5 and HTA6cl7 with a reduced tumorigenic potential exhibited only two copies of chromosome 20 (Tables 2 and 3).

Besides these differences, common chromosomal changes were observed in cell lines originating from different irradiation experiments. Loss of 13cen-q21 occurred in each irradiated cell line and, thus, independently in three different irradiation experiments. Loss of 8q23 as well as gain of 1q32-qter and 2q11.2-q14.1 were visible in HTG1 and HTA6 clones (Table 3).

DISCUSSION

The malignant transformation of human epithelial cells in vitro by the combined action of the DNA tumor virus SV40 and ionizing γ- and α-radiation is paralleled by cytogenetic changes. Previous reports of in vitro systems developed to study single steps of radiation-induced neoplastic transformation of epithelial cells [1,2,5,21] already postulated a multistep process for cancer development. It is associated with chromosomal alterations that were also detected in our in vitro system to investigate the radiation-induced transformation of the thyroid epithelium [4,6,7,14]. To search for specific changes attributable to immortalization, radiation

Table 1. Clonal Marker Chromosomes in HTori Cell Lines Analyzed by SKY

Marker	Chromosomal composition	Marker	Chromosomal composition
M1	der(1)(1pter→q44::5q31→qter)	M41	der(12)(12pter→q13::20p11→pter)
M2	der(1)(1pter→q44::9q11→qter)	M42	der(13)(9pter→p11::13p11→qter)
M3	der(1)(20pter→p11::1p11→qter)	M43	dic(14:20)(20pter→q11::14p?→qter)
M4	der(1)(1pter→q11::various chromosomes)	M44	der(14)(21qter→q11::14p11→qter)
M5	der(1)(1qter→p11::various chromosomes)	M45	der(14)(14qter→p?::1p11→pter)
M6	der(1)(1q21→pter::15qter→q22)	M46	der(14)(1qter→1q11::14p?→14q32::17q21→qter)
M7	del(2)(:p23→qter)	M47	der(15)(21qter→q11::15p11→qter)
M8	i(2)(qter→q10::q10→qter)	M48	der(15)(17pter→p11::15p?→qter)
M9	der(2)(2qter→p11::3q11→q26::7p?q?)	M49	der(15)(7pter→p11::15p?→qter)
M10	der(2)(2pter→q11::6q16→qter)	**M50**	del(16)(pter→q11:)
M11	der(2)(2qter→p11::10p?q?)	**M51**	der(16)(16qter→16p13::6p22→pter)
M12	der(3)(7qter→q22::3p25→q25::4p15::3q25→qter)	**M52**	der(17)(17pter→q25::3p?q?)
M13	der(3)(8qter→q?::3p11→qter)	**M53**	der(17)(17qter→p11::8q?::11q14→q23::Xp?q?::19p?q?::16p12→pter)
M14	der(3)(1qter→q32::12q14→q12::19p?q?::2q14→q11.2::3p11→qter)	**M54**	der(17)(11qter→q13::17p13→q11::8q?11q14→q23::Xp?q?::19p?q?::16p12→pter)
M15	der(4)(4p?q?::4p16→q32:)	M55	i(18)(qter→q10::q10→qter)
M16	der(4)(10qter→q11::4p15→qter)	**M56**	del(18)(pter→p21:)
M17	der(4)(20qter→q11::4p14→qter)	**M57**	del(18)(:p11→qter)
M18	del(5)(pter→q11:)	**M58**	der(19)(19pter→q13::1q?)
M19	der(5)(5qter→q21::5p15→qter)	**M59**	der(19)(19pter→q13::5p?q?)
M20	der(5)(5qter→p15::8q?::14p11→qter)	**M60**	der(19)(19pter→q13::11q13→qter)
M21	der(5)(5qter→p15::8q?::6q15→q23::8q?::14p11→qter)	M61	der(19)(19qter→p13::22q11→q12::17q22→qter)
M22	del(6)(pter→q13:)	M62	der(20)(20pter→q11::12q11→12qter)
M23	del(6)(pter→q15:)	M63	der(20)(19pter→q11::20q11→pter)
M24	der(6)(pter→q15::12p?q?)	M64	der(20)(20pter→q11::3p?q?::21q11→qter)
M25	der(6)(6pter→q21::2p21→pter)	M65	der(20)(20qter→p13::16p?q?::14q11→qter)
M26	der(6)(9pter→p11::6q11→pter)	M66	der(20)(:17q23→q11::20q11→p13::16p?q?::14q→qter)
M27	der(6)(6pter→q27::16q11→qter)	M67	der(20)(20qter→20p13::5p?q?::14q11→qter)
M28	der(7)(7pter→q32::10q11→qter)	**M68**	i(21)(qter→q10::q10→qter)
M29	der(7)(7pter→q11::20p12→pter)	**M69**	der(21)(21qter→p11::5q12→5qter)
M30	der(7)(7pter→q11::22q11→qter)	**M70**	der(21)(21qter→p11::10q22→qter)
M31	i(8)(qter→q10::q10→qter)	**M71**	der(21)(20pter→p11::21p11→qter)
M32	der(9)(9pter→q33::13q22→qter)	M72	der(21)(17pter→p11::21p11→qter)
M33	der(9)(21qter→q11::9p11→qter)	M73	der(21:22)(21qter→p11::22p11→q12::17q22→pter)
M34	der(9)(9qter→p11::15q11→qter)	M74	der(22)(22qter→p11::10p?q?::18q11→qter)
M35	der(10)(4pter→p15::10p11→pter)	**M75**	der(22)(22p13→q12::17q22→qter)
M36	del(11)(pter→q21:)	**M76**	der(22)(17qter→q22::22q12→p11::9q12→q33::13q22→qter)
M37	der(11)(:11p11→qter)	M77	der(22)(22qter→p11::18q11→qter)
M38	i(11)(qter→q10::q10→qter)	M78	der(22)(17qter→q22::22q12→p11::11q11→qter)
M39	dic(11;19)(19qter→p13::11p11→qter)	**M79**	der(X)(10pter→p11::Xq11→pter)
M40	der(11)(11pter→q13::Xq11→qter)		

Bold and single underline, markers of SV40 immortalization.

effects, and/or tumorigenicity, we compared chromosomal markers among the cell lines presented in Figure 1. The parental cell line HTori-3 [14] with cytogenetic alterations obviously related to SV40 immortalization served as starting point for a comparison with radiation-induced tumorigenic cell lines. Primary cultures from tumors developed in athymic nude mice (HTG1, HTA3, HTA6; Fig. 1) provided information on chromosomal changes induced by different doses of two radiation qualities in addition to alterations that developed during the process leading to tumorigenicity. To identify aberrations that are indispensable for the tumorigenic process, clones from the primary cultures of the tumors were rechecked for tumorigenicity (HTG1cl1, HTG1cl3, HTA3cl3, HTA6cl2, HTA6cl4, HTA6cl5, HTA6cl6, HTA6cl7, HTA6cl9; Fig. 1).

The G-banding analysis of the parental cell line HTori-3 suggested that polyploidization and marker chromosomes already originated during the SV40-mediated immortalization step. Karyotypic instability after SV40 integration preceding neoplastic transformation has previously been demonstrated for human fibroblasts [22]. Recurrent and more likely important markers for immortalization are represented by M1, M2, M12, M14, M20, M32, M36, M40, M51, M53, and M79 because they occurred in almost every cell line investigated (Table 2, Fig. 2). In addition, CGH revealed numerous

Table 2. Clonal Karyotypes of HTori Cell Lines Analyzed by SKY

	HTori-3	HTG1-clone1	HTG1-clone3	HTA3-clone3
Chromosome number	67–70	62–65	62–67	97–122
Ploidy range	3n–[a]	3n–[a]	3n–[b]	5n±[b]
Chromosome 1	1:M1;M2	1:M1;M2	1:1:M1;M2	1:1:M1;M6
Chromosome 2	2:2:2:M10;M11	2:2:2	2:2:2	2:2:M8;M9
Chromosome 3	3:3:M12;M14	3:M12;M14	3:M12;M14	3:3:M12;M13
Chromosome 4	4:4:4	4:4:M16	4:4:M16	4:4:4:4:4
Chromosome 5	5:5:M20	5:5:M20	5:5:M20	5:5:M18;M19;M20
Chromosome 6	6:6:M24	6:6:M26;M27	6:6:M26;M27	6:6:6:M22;M25
Chromosome 7	7:7:7:M28	7:7:M30	7:7:M30	7:7:7:7:7:7
Chromosome 8	8:8	8:8	8:8	8:8:8:8:8:M31
Chromosome 9	9:9:M32	9:M32	9:M32	9:9:M32;M34
Chromosome 10	10:10:10	10:10:M35	10:10:M35	10:10:10
Chromosome 11	11:M36;M37;M40	M36;M39;M40	M36;M39;M40	11:11:M36;M38
Chromosome 12	12:12:12	12:12:M41	12:12:M41	12:12:12:12
Chromosome 13	13:13:13	13:13	13:13	13:13:13:13:M42
Chromosome 14	14:14	14:14	14:14	14:14
Chromosome 15	15:15:15	15:15:M47	15:15:15	15:15
Chromosome 16	16:M50;M51	16:M50;M51	16:M50;M51	16:16:16:M51
Chromosome 17	17:M53	17:M52M53	17:M52:M53	17:17:17:M53
Chromosome 18	18:18:M56	18:18:M56	18:M56	18:18:18
Chromosome 19	19:M58;M59	19	19	19:19:19:M60
Chromosome 20	20:20:20:20	20:20:20:20:20:M64	20:20:20:20:20	20:20:20:20:20:20:M62
Chromosome 21	21:21:21:M68,M70	21:21:M68	21:21:M71	21:21:21:M69
Chromosome 22	22:22:22:M75	22:22:M75	22:22:M75	22:22:22
X chromosome	X:X:M79	X:M79	X:M79	X:X

chromosomal imbalances in HTori-3 (Table 3), which might be attributed to the immortalization process. Of special interest is the finding of loss of 6q material. SEN6, a locus for SV40-mediated immortalization of human cells, maps to 6q26-q27, and has been demonstrated to be deleted in SV40 immortalized cells [23]. Experiments using micro-cell-mediated chromosome transfer demonstrated that chromosomes 1, 2, 4, 6, 7, and 11 can confer senescence in various tumor cell lines [24–30]. It is further known that chromosome 11q is a strong candidate region for proto-oncogenes playing a key role in immortalization of keratinocytes upon transfection with human papillomavirus [31]. In our in vitro model system, chromosomes 1q, 4, 6, and 11 were found frequently affected by translocations as well as by numerical imbalances (Fig. 2, Table 3), suggesting that such changes occur during immortalization preceding tumorigenicity. It was assumed that inactivation due to chromosomal alterations of genes controlling cellular senescence can activate the process of immortalization [32]. Our SKY and CGH data on HTori-3 cells demonstrated that other immortalization-related, so far nonreported aberrations affected chromosomes 3p, 8p, 9p, 16p, 19q, 21, 22, which might harbor genes important for the immortalization process. Thus, this data can serve as a starting point for further microcell-mediated

assays to investigate their role in senescence and immortalization.

The original tumor cell lines (HTG1, HTA3, HTA6) exhibited extensive chromosomal instability (data not shown), which was less prominent in clones derived from these cell lines. We therefore decided to interpret only data originating from the cloned cell lines. Whereas markers M16, M26, M27, M30, M35, M39, M41, and M52 became apparent only in the γ-ray-induced lines (HTG1cl1 and HTG1cl3), markers M6, M8, M15, M17, M18, M21, M34, M69, and M72 were detected only in the α-ray-induced lines (HTA3cl3 and HTA6 clones). A similar observation was made by CGH analysis, which revealed losses on 1q and 2 as well as gains on 3q and 9p in HTA3cl3 only. If HTA3cl3 and HTA6 clones were compared following SKY analysis, it was observed that M6, M8, M18, M34, and M69 appear only in HTA3cl3, while M15, M17, M21, and M72 occurred exclusively in HTA6 clones. The copy numbers for chromosomes 7, 8, and 12 were also different between HTA3cl3 and HTA6 clones. If clones 1 and 3 of HTG1 cell line were compared, only small differences became apparent, probably reflecting a clonal evolution of tumor cells. Also, HTA6 clones 2, 4, 5, 6, 7, and 9 were very similar in their aberration pattern, although there were more extensive alter-

Table 2.   Continued

	HTA6-clone2	HTA6-cloned4	HTA6-clone5	HTA6-clone6	HTA6-clone7	HTA6-clone9
Chromosome	59–64	59–68	57–64	59–64	58–61	60–63
Ploidy range	3n–[a]	3n–[a]	3n–[a]	3n–[a]	3n–[a]	3n–[a]
Chromosome 1	1:M1;M2	M2;M3;M4;M5	1:M1;M2	1:M1;M2	1:M1;M2	1:M1;M2
Chromosome 2	2:2:2	2:2:2	2:2:2	2:2:2	2:2:M7	2:2:2
Chromosome 3	3:M12;M14	3:M12;M14	3:M12;M14	3:M12;M14	3:M12;M14	3:M12;M14
Chromosome 4	4:M15;M17	4:M15;M17	4:M15;M17	4:M15;M17	4:M15;M17	4:M15;M17
Chromosome 5	5:5:M21	5:5:M21	5:5:M21	5:5:M18;M21	5:5:M21	5:5:M21
Chromosome 6	6:M22;M23	6:6:M23	6:6:M23	6:6:M23	6:6:M22	6:6:M23
Chromosome 7	7:7	7:7:7:7	7:7:M29	7:7:M29	7:7:M29	7:7:M29
Chromosome 8	8:8	8:8	8:8	8:8	8:8	8:8
Chromosome 9	9:M32	9:M32;M33	9:M32	9:M32	9:M32	9:M32
Chromosome 10	10:10	10:10:10	10:10:10	10:10	10:10:10	10:10:10
Chromosome 11	M36;M37;M40	M36;M40	M36;M37;M40	M36;M37;M40	M36;M37;M40	M36;M37;M40
Chromosome 12	12:12	12:12	12:12	12:12	12:12	12:12
Chromosome 13	13:13	13:13	13:13	13:13	13:13	13:13
Chromosome 14	14:14:M44	M45;M46	14	14:14	14:14	14:M43
Chromosome 15	15:15:15	15:M48;M49	15:15:15	15:15:15	15:15:15	15:15:15
Chromosome 16	16:16:M50;M51	16:M50;M51	16:M50,M51	16:M50;M51	16:M50;M51	16:M50;M51
Chromosome 17	17:M53	17:M54	17:M53	17:M53	17:M53	17:M53
Chromosome 18	18:M56	18:18:M56	18	18:M56;M57	18	18:M55;M56
Chromosome 19	19	19	19:M61	19	19	19
Chromosome 20	20:20:20:20:M63	20:20:20:20:M63	20:20;M63;M67	20:20:20:20:M63;M67	20:20;M63;M66	20:20:M63;M65
Chromosome 21	21:21:M68;M72	21:21:M72	21:21:M68;M72	21:21:M68;M72	21:21:M68;M72	21:M68:M72
Chromosome 22	22:22:M75	22:22:M75	22:M75;M76;M77	22:22:M73;M75;M76;M78	22:M74;M76	22:M76
X chromosome	X:M79	X:M79	X:M79	X:M79	X:M79	X:M79

Bold, marker chromosomes; single underline, markers of SV40 immortalization; dotted underline, markers characteristic for γ-ray-induced line; double underline, markers characteristic for α-ray-induced lines

[a] 3n-, hypotriploid cell line.

[b] 5n±, near-pentaploid cell line

ations than between the HTG clones. Some of these different aberrations might be responsible for the varying tumorigenic behavior of the HTA6 clones. Moreover, it appeared that deletions on chromosomes 9q32-q34 and 7q21-q31 as well as increased copy numbers of chromosome 20 were important for the tumorigenic phenotype. According to our data, it seems that varying combinations of these three aberrations could contribute to a more aggressive tumorigenic behavior. This is concordant with findings in a variety of solid-tumor entities that frequently exhibit losses on 7q21-q31 and 9q32-q34 as well as a gain of chromosome 20 [33–35]. It can be further assumed that common aberrations among radiation-induced lines (loss on 8q23 and 13cen-q21, gain on 1q32-qter and 2q11.2-q14.1) are strong indicators for the involvement of genes located within these regions in radiation-induced tumor development in thyroid epithelial cells. Although they probably imply significant genetic changes, it is likely that they were not sufficient to cause the aggressive malignant phenotype since they occurred also in the nontumorigenic lines. It is, however, of interest that recent CGH and loss of heterozygosity (LOH) studies on follicular carcinomas [36,37] and Hürthle cell tumors [38] of the

thyroid gland revealed the same aberrations (losses on chromosomes 13q and 9q31-q33, gains on chromosomes 1q and 20) as this model cell system of radiation-induced transformation of epithelial thyroid cells.

A comprehensive breakpoint analysis of chromosomal aberrations in HTori lines (Fig. 4) and in radiation-induced childhood thyroid tumors from Belarus [10] revealed coinciding mapped breakpoints on chromosomes 1q, 4q, 5q, 6, 7q, 9q, 10q, 11q, 12q, 15q, 16, and 22q. However, some clustered chromosomal breakpoints observed in HTori lines on chromosome 21 and most prevalently on chromosome 20 were different from the Belarussian tumors. These findings indicate that radiation-induced thyroid tumors might share some hot spots of chromosomal damage. Different doses and radiation qualities may have led to variations in the aberration pattern.

In conclusion, we demonstrate specific chromosomal aberrations associated with SV40 immortalization and radiation-induced transformation of human epithelial thyroid cells. The data are in line with previous reports describing immortalization-related changes in epithelial cells but also indicate newly identified chromosomal markers originating
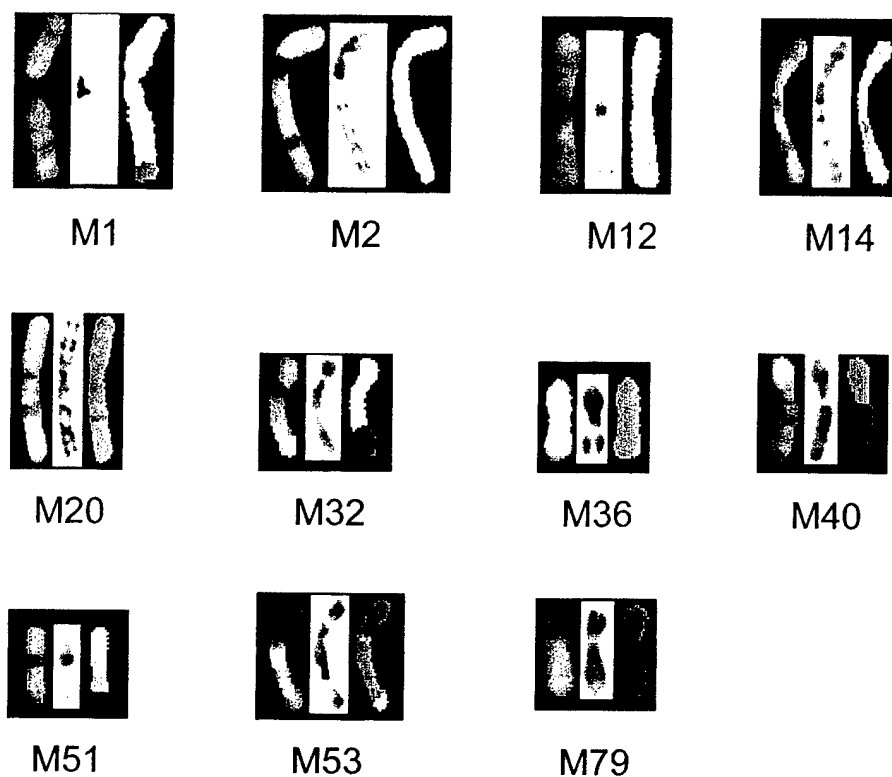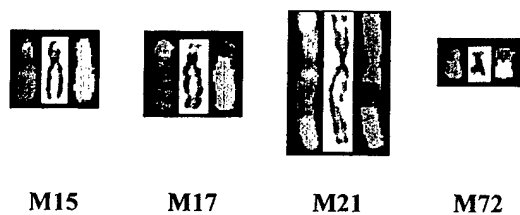
Fig. 2. Chromosomal markers of SV40 immortalization detected by SKY. Markers M1, M2, M12, M14, M20, M32, M36, M40, M51, M53, and M79 are shown as RGB image, DAPI-banded image, and classified image in pseudocolors (from left to right). The structural composition of each marker chromosome is indicated in Table 1.

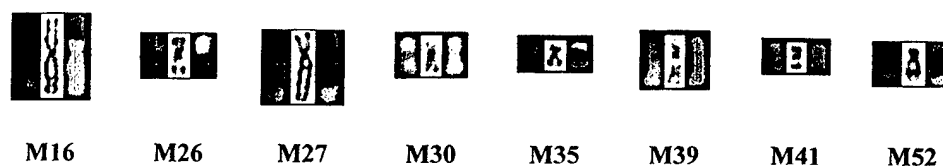## A HTA3 cell lines

B HTA6 cell lines

C HTG1 cell lines

Fig. 3. Chromosomal markers of different HTori cell lines. Specific markers of HTA3 clones (**A**), HTA6 clones (**B**), and HTG1 clones (**C**) are demonstrated as RGB image, DAPI-banded image, and classified image in pseudocolors (from left to right). The chromosomal composition of each marker is indicated in Table 1.
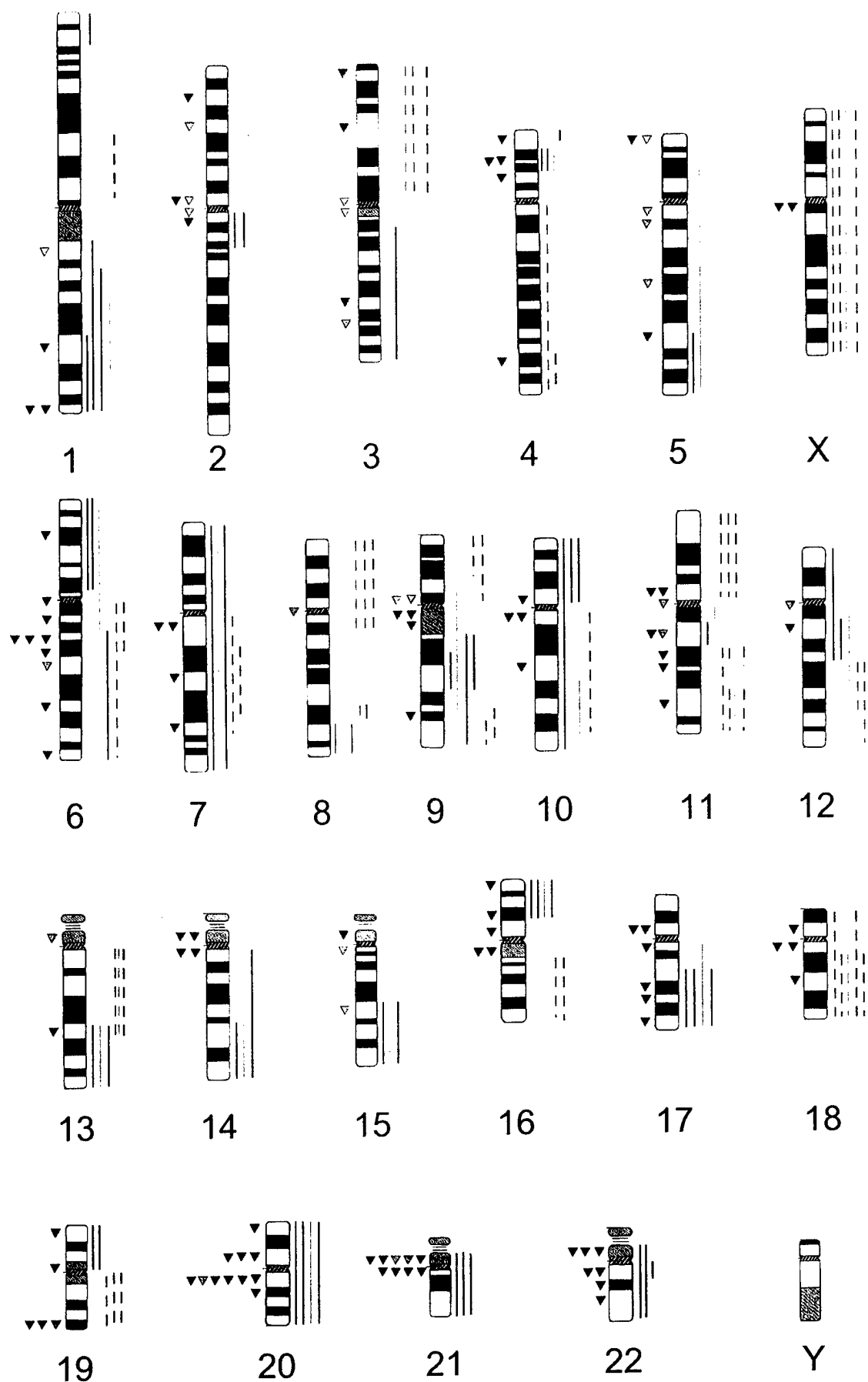
Fig. 4. Breakpoints of structural chromosome aberrations and chromosomal gains and losses in different HTori cell lines. They were indicated for the individual cell lines in different colors (blue, HTori-3; green, HTG1; grey, HTA3; red, HTA6). Breakpoints of structural aberrations are shown on the left side of each ideogram. On the right side of each ideogram, gains are represented by running lines and losses by dashed lines.

Table 3. CGH Results of 10 HTori Cell Lines

Cell line	Gains	Losses
HTori-3	4p15, 5, 6p12-pter, 7, 8q24.1-qter, 9q21-q22, 10, 11q13, 12pter-q15, 13q22-qter, 14q24-qter, 15q22-qter, 16p12-pter, 17q21-qter, 19p, 20 (a: 20q13), 21, 22	3p, 4q, 6q, 8pter-q21.2, 9p21-pter, 11cen-p15, 11q14-qter, 12q21-q23, 16q, 18, 19q, X
HTG1-clone1	1q32-qter, 2q11.2-q14.1, 4p15, 5q31-qter, 6p, 10p, 12q13-q15, 16p12-pter, 17q21-qter, 20 (a: 20p13), 21, 22	3p, 7cen-q32, 8pter-q21, 8q23, 9q34, 11cen-p15, 11q14, 11q23-qter, 12q21-qter, 13cen-q22, 18q21-qter, 19q, X
HTG1-clone3	1q32-qter, 2q11.2-q14, 4p15, 5q31-qter, 6p, 10p, 12q13-q15, 16p12-pter, 17q21-qter, 20 (a: 20p13), 21, 22	3p, 7cen-q32, 8pter-q21, 8q23, 9q34, 11cen-p15, 11q14, 11q23-qter, 12q21-qter, 13cen-q22, 18q21-qter, 19q, X
HTA3-clone3	3q13-qter, 4p15, 5, 6pter-q14 (a: 6p23-pter), 7 (a: 7q32-qter), 8 (a: 8q22, 8q24), 9p12-p21, 9q21-qter, 10q23-qter, 11q12-q13, 12q12-q21, 13q22-qter, 14q24-qter, 15q22-qter, 16p12-pter, 17q, 20 (a: 20p13, 20q13)	1cen-q41, 2, 3p, 11q23-qter, 13cen-q22, 18q, X
HTA6-clone2	1p34.1-pter, 1q32-qter, 2q11.2-q14.1, 5q31-qter, 6p22-pter, 8q24, 16p11.2-pter, 17q21-qter, 19p, 20, 21, 22q11.2	3p, 4p16, 4q32-qter, 6q12-q16, 7p21-q31, 8pter-q21, 8q23, 9p, 9q32-q34, 10cen-q25, 11cen-p15, 11q14, 11q23-qter, 12p, 12q15-qter, 13cen-q21, 19q, X
HTA6-clone4	1q, 2q11.2-q14.1, 6p22-pter, 7, 8q24, 9q, 10p, 14q, 16p11.2-pter, 17q21-qter, 20, 21, 22q11.2	1p13-p22, 3p, 4p16, 4q32-qter, 8pter-q21, 8q23, 9p, 11cen-p15, 11q14, 11q23-qter, 12p, 12q15-qter, 13cen-q21, 16q, 18q21-qter, 19q, X
HTA6-clone5	1q32-qter, 2q11.2-q14.1, 5q31-qter, 6p22-pter, 8q24, 9q21-q22, 10p, 13q22-qter, 14q, 15q22-qter, 16p11.2-pter, 17q21-qter, 20, 21, 22q11.2	3p, 4p16, 4q32-qter, 7q21-q31, 8pter-q21, 8q23, 9p, 11cen-p15, 11q14, 11q23-qter, 12p, 12q15-qter, 13cen-q21, 16q, 18, 19q, X
HTA6-clone6	1q32-qter, 2q11.2-q14.1, 5q31-qter, 6p22-pter, 8q24, 9q21-q22, 10p, 13q22-qter, 14q, 16p11.2-pter, 17q21-qter, 20, 21, 22q11.2	3p 4p16, 4q32-qter, 7q21-q31, 8pter-q21, 8q23, 9p, 9q32-q34, 11cen-p15, 11q14, 11q23-qter, 12p, 12q15-qter, 13cen-q21, 16q, 18, 19q, X
HTA6-clone7	1q32-qter, 2q11.2-q14.1, 5q31-qter, 6p22-pter, 8q24, 9q21-q22, 10p, 13q22-qter, 14q, 15q22-qter, 16p11.2-pter, 17q21-qter, 19p, 20, 21, 22q11.2	3p, 4p16, 4q32-qter, 7q21-q31, 8pter-q21, 8q23, 9p, 11cen-p15, 11q14, 11q23-qter, 12p, 12q15-qter, 13cen-q21, 16q, 18, X
HTA6-clone9	1q32-qter, 2q11.2-q14.1, 5q31-qter, 6p22-pter, 8q24, 9q21-q22, 10p, 13q22-qter, 14q, 15q22-qter, 16p11.2-pter, 17q21-qter, 20, 21, 22q11.2	3p, 4p16, 4q32-qter, 7q21-q31, 8pter-q21, 8q23, 9p, 11cen-p15, 11q14, 11q23-qter, 12p, 12q15-qter, 13cen-q21, 16q, 18p11.3, 19q, X

a. Amplification
Bold and single underline, markers of SV40 immortalization.

from this process. The identification of radiation-induced chromosomal changes in the tumorigenic cell lines by use of advanced molecular cytogenetic techniques such as SKY and CGH strongly supports the usefulness of the established epithelial cell lines as in vitro model for studying important steps during radiation-induced malignant transformation in human thyroid cells.

ACKNOWLEDGMENTS

REFERENCES

1. Rhim JS, Yoo JH, Park JH, Thraves P, Salehi Z, Dritschilo A. Evidence for the multistep nature of in vitro human epithelial cell carcinogenesis. Cancer Res 1990;50:5653–5657.

2. Thraves P, Salehi Z, Dritschilo A, Rhim JS. Neoplastic transformation of immortalized human epidermal keratinocytes by ionizing radiation. Proc Natl Acad Sci USA 1990;87:1174–1177.

3. Hei TK, Piao CQ, Willey JC, Thomas S, Hall EJ. Malignant transformation of human bronchial epithelial cells by radon-simulated alpha-particles. Carcinogenesis 1994;15:431–437.

4. Riches AC, Herceg Z, Bryant PE, Wynford-Thomas D. Radiation-induced transformation of SV40-immortalized human thyroid epithelial cells by single and fractionated exposure to gamma-irradiation in vitro. Int J Rad Biol 1994;66:757–765.

5. Kuettel MR, Thraves PJ, Jung M, Varghese SP, Prasad SC, Rhim JS, Dritschilo A. Radiation-induced neoplastic transformation of human prostate epithelial cells. Cancer Res 1996;56:5–10.

6. Riches AC. Herceg Z. Bryant PE. Stevens DL. Goodhead DT. Radiation-induced transformation of SV40-immortalized human thyroid epithelial cells by single exposure to plutonium alpha-particles in vitro. Int J Rad Biol 1997;72:515–521.

7. Riches A. Herceg Z. Wang H. Bryant P. Armitage M. Gamble S. Arrand J. O'Reilly S. Seymour C, Mothersill C. Radiation-induced carcinogenesis: studies using human epithelial cell lines. Radiat Oncol Invest 1997;5: 139–143.

8. Ried T. Liyanage M. du Manoir S. Heselmeyer K. Auer G. Macville M. Schröck E. Tumor cytogenetics revisited: Comparative genomic hybridization and spectral karyotyping. J Mol Med 1997;75:801–814.

9. Macville M. Schröck E. Padilla-Nash H. Keck C. Ghadimi BM. Zimonjic D. Popescu N. Ried T. Comprehensive and definitive molecular cytogenetic characterization of HeLa cells by spectral karyotyping. Cancer Res 1999;59:141–150.

10. Zitzelsberger H. Lehmann L. Hieber L. Weier H-UG. Janish C. Fung J. Negele T. Spelsberg F, Lengfelder E. Demidchik EP. Salassidis K. Kellerer AM, Werner M. Bauchinger M. Cytogenetic changes in radiation induced tumors of the thyroid. Cancer Res 1999;59:135–140.

11. Veldman T. Vignon C. Schröck E. Rowley JD. Ried T. Hidden chromosome abnormalities in haematological malignancies detected by multicolour spectral karyotyping. Nat Genet 1997;15:406–410.

12. Rowley JD. Reshmi S. Carlson K. Roulston D. Spectral karyotype analysis of T-cell acute leukemia. Blood 1999;93:2038–2042.

13. Kallioniemi A. Kallioniemi O. Sudar D, Rutovitz D. Gray JW. Waldman F. Pinkel D. Comparative genomic hybridization for molecular cytogenetic analysis of solid tumors. Science 1992;258:818–821.

14. Lemoine NR. Mayall ES. Jones T, Sheer D, McDermid S. Kendall-Taylor P. Wynford-Thomas D. Characterisation of human thyroid epithelial cells immortalised in vitro by simian virus 40 DNA transfection. Br J Cancer 1989;60:897–903.

15. Mitelman F. ed. ISCN: An International System for Human Cytogenetic Nomenclature. Basel: S. Karger, 1995.

16. Schröck E. du Manoir S, Veldman T, Schoell B, Wienberg J. Ferguson-Smith MA, Ning Y, Ledbetter DH, Bar-Am I. Soenksen D, Garini Y, Ried T. Multicolor spectral karyotyping of human chromosomes. Science 1996;273:494–497.

17. Garini Y. Macville M, du Manoir S, Buckwald RA, Lavi M. Katzir N. et al. Spectral karyotyping. Bioimaging 1996;4:65–72.

18. Kallioniemi OP. Kallioniemi A, Piper J, Isola J, Waldman FM. Gray JW, Pinkel D. Optimizing comparative genomic hybridization for analysis of DNA sequence copy number changes in solid tumors. Genes Chromosomes Cancer 1994;10:231–243.

19. Bruch J. Wöhr G, Hautmann R, Mattfeldt T, Brüderlein S. Möller P. Sauter S. Hameister H. Vogel W, Paiss T. Chromosomal changes during progression of transi-

tional cell carcinoma of the bladder and delineation of the amplified interval on chromosome arm 8q. Genes Chromosomes Cancer 1998;23:167–174.

20. Solinas-Toldo S. Wallrapp C. Müller-Pillasch F. Bentz M. Gress T. Lichter P. Mapping of chromosomal imbalances in pancreatic carcinoma by comparative genomic hybridization. Cancer Res 1996;56:3803–3807.

21. Hukku B. Thraves P. Dritschilo A. Rhim JS. Chromosomal changes observed in immortalized human keratinocytes transformed by ionizing radiation. Cancer Genet Cytogenet 1997;93:125–139.

22. Ray FA. Peabody DS. Cooper JL. Cram LS, Kraemer PM. SV40 T antigen alone drives karyotype instability that precedes neoplastic transformation of human diploid fibroblasts. J Cell Biochem 1990;42:13–31.

23. Banga SS. Kim S. Hubbard K. Dasgupta T, Jha KK. Patsalis P. Hauptschein R. Gamberi B. Dalla-Favera R, Kraemer P. Ozer HL. SEN6. a locus for SV40-mediated immortalization of human cells. maps to 6q26-27. Oncogene 1997;14:313–321.

24. Sugawara O. Oshimura M. Koi M. Annab LA, Barrett JC. Induction of cellular senescence in immortalized cells by human chromosome 1. Science 1990;247:707–710.

25. Ning Y. Weber JL. Killary AM. Ledbetter DH, Smith JR. Pereira-Smith OM. Genetic analysis of indefinite division in human cells: Evidence for a cell senescence-related gene(s) on human chromosome 4. Proc Natl Acad Sci 1991;88:5635–5639.

26. Koi M. Jahnson LA. Kalikin LM, Little PF, Nakamura Y. Feinberg AP. Tumor cell growth arrest caused by subchromosomal transferable DNA fragments from chromosome 11. Science 1993;260:361–364.

27. Ogata T. Ayusawa D, Namba M, Takahashi E, Oshimura M. Oishi M. Chromosome 7 suppresses indefinite division of nontumorigenic immortalized human fibroblast cell lines KMST-6 and SUSM-1. Mol Cell Biol 1993;13:6036–6043.

28. Hensler PJ, Annab LA. Barrett JC, Pereira-Smith OM. A gene involved in control of human cellular senescence on human chromosome 1q. Mol Cell Biol 1994; 14:2291–2297.

29. Sandhu AK. Hubbard K. Kaur GP, Jha KK, Ozer HL, Athwal RS. Senescence of immortal human fibroblasts by the introduction of normal human chromosome 6. Proc Natl Acad Sci USA 1994;91:5498–5502.

30. Uejima H, Mitsuya K, Kugoh H, Horikawa I, Oshimura M. Normal human chromosome 2 induces cellular senescence in the human cervical carcinoma cell line SiHa. Genes Chromosomes Cancer 1995;14:120–127.

31. Solinas-Toldo S, Dürst M. Lichter P. Specific chromosomal imbalances in human papillomavirus-transfected cells during progression toward immortality. Proc Natl Acad Sci USA 1997;94:3854–3859.

32. Sasaki M. Honda T. Yamada H, Wake N, Barrett JC,

Oshimura M. Evidence for multiple pathways to cellular senescence. Cancer Res 1994;54:6090–6093.

33. Mitelman F, ed. Catalog of Chromosome Aberrations in Cancer. New York: Wiley-Liss. 1998.

34. Knuutila S, Bjorkqvist AM, Autio K, Tarkanen M, Wolf M, Monni O, Szymanska J, Larramendy ML, Tapper J, Pere H, El-Rifai W, Hemmer S, Wasenius VM, Vidgren V, Zhu Y. DNA copy number amplifications in human neoplasms: Review of comparative genomic hybridization studies. Am J Pathol 1998;152: 1107–1123.

35. Knuutila S, Aalto Y, Autio K, Björkqvist AM, El-Rifai W, Hemmer S, Huhta T, Kettunen E, Kiuru-Kuhlefelt S, Larramendy ML, Lushnikova T, Monni O, Pere H, Tapper J, Tarkkanen M, Varis A, Wasenius VM, Wolf

M, Zhu Y. DNA copy number losses in human neoplasms. Am J Pathol 1999;155:683–694.

36. Tung WS, Shevlin DW, Kaleem Z, Tribune DJ, Wells SA Jr, Goodfellow PJ. Allelotype of follicular thyroid carcinomas reveals genetic instability consistent with frequent nondisjunctional chromosomal loss. Genes Chromosomes Cancer 1997;19:43–51.

37. Hemmer S, Wasenius VM, Knuutila S, Franssila K, Joensuu H. DNA copy number changes in thyroid carcinoma. Am J Pathol 1999;154:1539–1547.

38. Tallini G, Hsueh A, Liu S, Garcia-Rostan G, Speicher MR, Ward DC. Frequent chromosomal DNA unbalance in thyroid oncocytic (Hürthle cell) neoplasms detected by comparative genomic hybridization. Lab Invest 1999;79:547–555.

REVIEW

DNA Fiber Mapping Techniques for the Assembly of High-resolution Physical Maps

Heinz-Ulrich G. Weier

Department of Subcellular Structure, Life Sciences Division, University of California, Ernest Orlando Lawrence Berkeley National Laboratory, Berkeley, California

SUMMARY High-resolution physical maps are indispensable for directed sequencing projects or the finishing stages of shotgun sequencing projects. These maps are also critical for the positional cloning of disease genes and genetic elements that regulate gene expression. Typically, physical maps are based on ordered sets of large insert DNA clones from cosmid, P1/PAC/BAC, or yeast artificial chromosome (YAC) libraries. Recent technical developments provide detailed information about overlaps or gaps between clones and precisely locate the position of sequence tagged sites or expressed sequences, and thus support efforts to determine the complete sequence of the human genome and model organisms. Assembly of physical maps is greatly facilitated by hybridization of non-isotopically labeled DNA probes onto DNA molecules that were released from interphase cell nuclei or recombinant DNA clones, stretched to some extent and then immobilized on a solid support. The bound DNA, collectively called "DNA fibers," may consist of single DNA molecules in some experiments or bundles of chromatin fibers in others. Once released from the interphase nuclei, the DNA fibers become more accessible to probes and detection reagents. Hybridization efficiency is therefore increased, allowing the detection of DNA targets as small as a few hundred base pairs. This review summarizes different approaches to DNA fiber mapping and discusses the detection sensitivity and mapping accuracy as well as recent achievements in mapping expressed sequence tags and DNA replication sites.

(J Histochem Cytochem 49:939–948, 2001)

HIGH-RESOLUTION PHYSICAL MAPS are indispensable for large-scale, cost-effective gene discovery. The construction of such maps of the human genome and model organisms therefore has been one of the major goals of the human genome project (Collins and Galas 1993). The most common physical mapping strategies implement a bottom-up approach for organizing individual inserts from large genomic libraries into a high-resolution map of contiguous overlapping fragments (contigs). The progress in cloning large, megabasepair (Mbp)-sized genomic DNA fragments in yeast artificial chromosomes (YACs) (Cohen et al. 1993; Olson

1993) has made it possible to rapidly construct low-resolution framework maps based on overlapping YAC clones. Fluorescence in situ hybridization (FISH) has proved indispensable for identification of non-chimeric YAC clones and for physical mapping of individual YAC clones onto metaphase chromosomes (Selleri et al. 1992). To generate physical maps with a resolution of 1 Mbp or better, the YAC clones are ordered by combining different complementing analytic techniques: pulsed-field gel electrophoresis (PFGE) (Vetrie et al. 1993), FISH with interphase cell nuclei or metaphase spreads (Trask et al. 1989; Brandriff et al. 1992; Ashworth et al. 1995), sequence tagged site (STS) content mapping (Green and Olson 1990; Coffey et al. 1992; Weissenbach et al. 1992; Lu–Kuo et al. 1994; Locke et al. 1996), and/or DNA repeat fingerprinting (Bellanné–Chantelot et al. 1992; Zucchi and Schlessinger 1992; Waterston and Sulston 1995; Bell et al. 1995).

Correspondence to: H.-U. Weier, Dept. of Subcellular Structure, Life Sciences Division, MS 74-157, U. of California, Lawrence Berkeley National Laboratory, 1 Cyclotron Road, Berkeley, CA 94720. E-mail: ulliweier@hotmail.com

High-resolution maps providing ordered sets of cloned DNA fragments at the 100-kb level of resolution are assembled with smaller, more manageable DNA fragments isolated from other libraries. Most groups prefer cloning of genomic DNA in vectors that maintain relatively large DNA fragments without re-arrangements, are non-chimeric, and allow easy DNA purification. In general, high-resolution maps are composed of overlapping cosmids (Stallings et al. 1992; Tynan et al. 1992; Nizetic et al. 1994), P1/PAC clones (Pierce et al. 1992; Ioannou et al. 1994), or bacterial artificial chromosomes (BACs) (Shizuya et al. 1992). Assembly of the high-resolution maps requires identification of cloned DNA sequences that contain overlapping regions of the genome (Cheng and Weier 1997). To minimize the effort invested in assembling a contiguous set of clones, clone overlaps need to be determined quickly and accurately. This has been accomplished by various forms of clone fingerprinting [e.g., by identification of common restriction fragment or inter-Alu PCR patterns (Branscomb et al. 1990; Nelson 1991; Patil et al. 1994), by hybridization to bound filter clone arrays (Hoheisel and Lehrach 1993; Locke et al. 1996) or oligonucleotide arrays (Sapolsky and Lipshutz 1996), and by identification of overlapping sequence tagged sites (Green et al. 1991; Aburatani et al. 1996). The development of radiation hybrid mapping (Cox et al. 1990), the availability of large numbers of STS markers, and the construction of extensive bacterial clone resources provide additional means to accelerate the process of mapping a chromosome and preparing clone contigs ready for sequencing. These techniques, although effectively used by the genome community, are limited because they do not readily yield information about contig orientation, extent of deletions or rearrangements in clones, overlap of contig elements, or their chimerism status, nor do they provide information about the extent of gaps in the maps. The precise localization of cloned DNA fragments within much larger genomic fragments and knowledge about the extent of overlap between two clones is needed to assemble high-resolution physical maps. Techniques to rapidly identify minimally overlapping clones and to determine the extent and orientation of overlap expedite the construction of minimal tiling paths and facilitate the sequence assembly process. As demonstrated in this review, FISH can provide this critical information. Furthermore, FISH-based mapping is one of the few mapping procedures without requirements for different clones to overlap to be positioned and ordered (Horelli–Kuitunen et al. 1999).

In early applications of FISH-based clone ordering and assembly of physical maps, Brandriff and colleagues (1991a) took advantage of the high hybridization efficiency and enhanced spatial resolution obtained with decondensed human sperm DNA. In their approach, individual human sperm nuclei were fused with hamster eggs and probes were hybridized to the decondensed DNA of human pronuclei (Brandriff et al. 1991b). The example in Figure 1B demonstrates such decondensation in form of a cloud or network of green signals produced by a biotin-labeled probe directed towards the repeated satellite III DNA in the heterochromatic region of chromosome 9q11. The probe visualized with avidin–FITC fluoresced in green (Figure 1B), and the DNA was counterstained with DAPI emitting blue fluorescence (Figure 1A). The human sperm–hamster egg fusion technique was used successfully to order cosmid clones in preparing high-resolution physical maps for human chromosome 19 (Brandriff et al. 1992; Ashworth et al. 1995).

Figure 1 DNA fiber mapping. (A,B) Hybridization to decondensed sperm nuclei DNA allows probes to be ordered with high resolution. (B) Results of hybridizing a biotinylated probe specific for the chromosome 9-specific satellite III DNA and detection of bound probe molecules with avidin-FITC. (A) DAPI-counterstained DNA. (C) DNA released from cell nuclei can be hybridized very efficiently with non-isotopically labeled probes. A biotinylated DNA probe specific for α-satellite repeats on chromosomes 13 and 21 generated hybridization signals that appear yellow due to overlap between the green probe fluorescence and the red fluorescence of propidium iodide, which was used to counterstain the DNA. (D–G) High-resolution mapping of α-satellite DNA domains using surface spreads of DNA fibers. Unfixed human white blood cells were spread on glass slides, fixed with acetic acid:methanol, and hybridized with a biotinylated probe for chromosome 13/21-specific alphoid DNA. Green signal (D,F) delineating the alphoid tandem repeats appear as beads-on-a-string in the more extended chromatin parts. Images of the propidium iodide-counterstained DNA (E,G) demonstrate hybridization tracks located in DNA fibers of very different size. (H) Lambda DNA molecules bound to an APS-derivatized glass slide were straightened by the receding meniscus during drying and hybridized with biotin- or digoxigenin-labeled restriction fragments which were detected with avidin–FITC (green) and rhodamine-conjugated antibodies against digoxigenin (red). (I) Circular DNA molecules were excised from a PFGE gel and purified by agarose digestion. A small plasmid probe of about 2 kb was mapped onto a single, closed circular BAC DNA molecule. An FITC-labeled probe mix (green) delineates the BAC vector. A small probe (~1200 bp) binds within the vector part near the T7 promoter (red). The BAC molecule was counterstained by hybridization of a probe detected with avidin conjugated to AMCA (blue). (J,K) The extent of overlap between clones can be determined rapidly by hybridizing one clone onto DNA fibers prepared from the other clone. Here, a BAC clone (red) was mapped onto a partially overlapping circular PAC molecule (blue). The vector part of about 16 kb was counterstained with green/red probe combination. The results are summarized schematically in K. (L) Hybridization of labeled cDNA (red signals on top of blue signals) onto DNA fibers prepared from genomic clones such as BACs reveals the position and genomic organization of expressed sequences. The BAC molecule was counterstained by hybridization of a probe detected with avidin conjugated to AMCA (blue). The vector part of about 8 kb was counterstained with green/red probe combination. Bars = 10 μm.

A B C D E F G H I J K L

BAC

PCR probe

17 kb

80 kb

PAC vector

T7 promoter

PAC
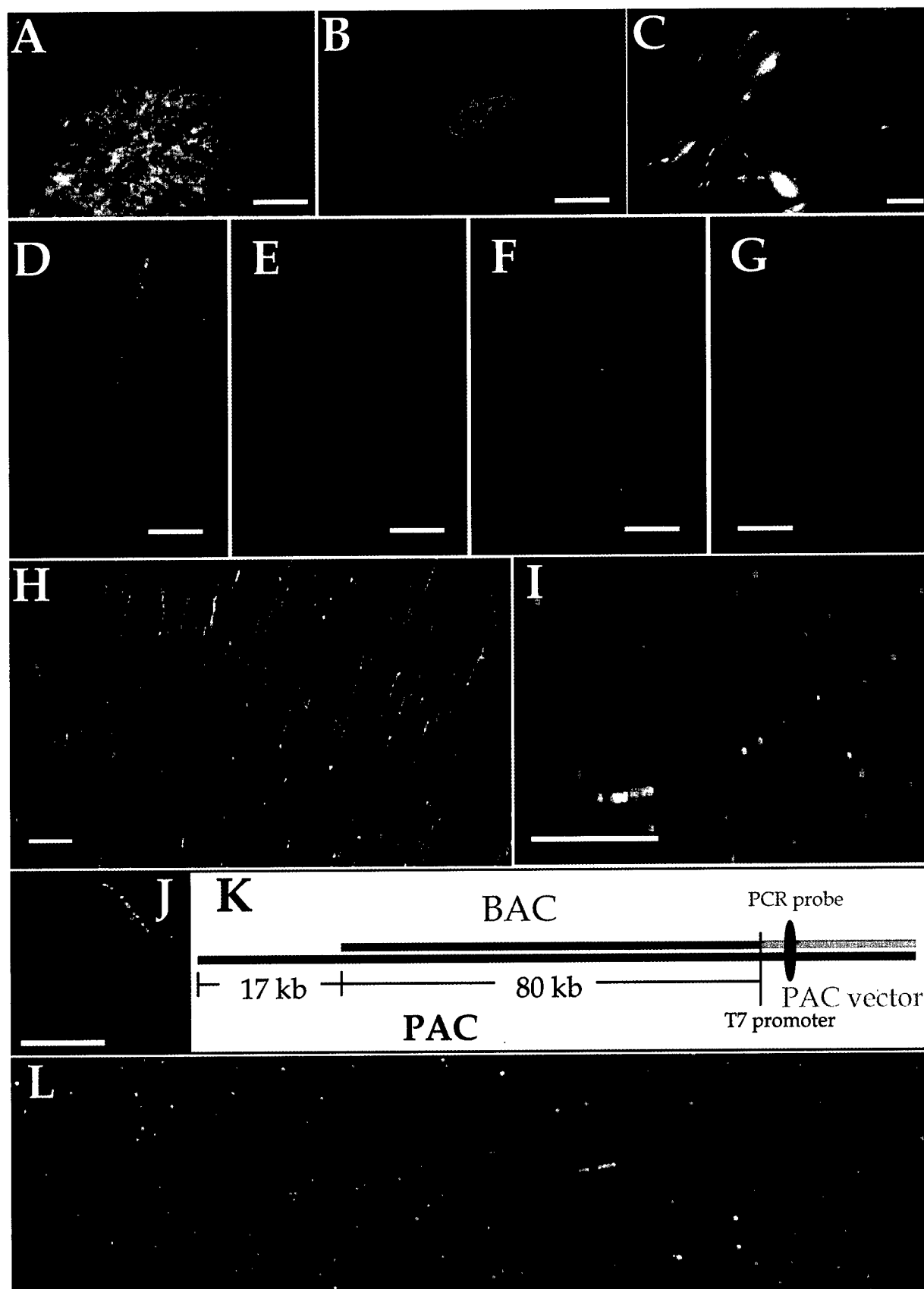
The procedure, however, had two obvious problems. Fusion of human sperm with hamster eggs and fixation of pronuclei is a time-consuming, laborious process and might not scale well enough to meet the high-throughput requirements of most genome projects. The second shortfall of the procedure was a complete lack of control over the extent of DNA decondensation and orientation of pronuclei. This spurred efforts in the 1990s to manipulate chromatin or purified DNA molecules that could serve as a template for high-resolution physical mapping of DNA probes. The optimal procedure would be inexpensive, rapid, reproducible, and deliver mapping data limited only by the resolution of the light microscope. A decade later, we find ourselves equipped with an arsenal of complementary FISH-based mapping procedures that cover a very broad range of mapping intervals. Furthermore, the simultaneous development of more sensitive fluorescence detection reagents has pushed the limits of detection down to a few hundred basepairs (bp).

DNA Fiber Mapping

The expression "DNA fiber mapping" has become a collective name for quite different mapping techniques. As indicated in Figure 2, the diameter of DNA fibers increases as DNA molecules with a diameter of 2 nm are packed into chromatin ranging from 10 nm for histone-packed DNA molecules and 30 nm for chromatin fibers all the way to chromatids of 700 nm diameter. Chromatin can be released from interphase cell nuclei by various chemical or mechanical methods, and investigators tried to coin names that reflect their individual approach. Isolation of DNA from cell nuclei, extension, and preparation of chromatin or DNA fibers with diameters ranging in size from a few to several hundred nm (Figure 2) improves the accessibility of the DNA targets for both probes and detection reagents. Accordingly, the hybridization efficiencies increase, and DNA targets of less than 1 kb can be detected routinely using procedures normally applied in metaphase and interphase cell FISH.

In 1992, Heng et al. described the use of chemicals to release chromatin from interphase cell nuclei. The results look somewhat similar to the propidium iodide-stained free chromatin shown in Figure 1C. Heng et al. (1992) used the drug N-[4-(9-acridinylamino)-3-methoxyphenyl]-methanesulfonamide (m-AMSA) and an alkaline lysis procedure to release the DNA from interphase cells and demonstrated mapping of DNA sequences in distances ranging from 21 kb to 350 kb onto the extended chromatin. The authors speculated that, with multicolor FISH, free chromatin mapping would readily resolve gene sequences separated by as little as 10 kb (Heng et al. 1992). Soon thereafter, Sen-

ger et al. (1994) and Fidlerova et al. (1994) demonstrated the use of a sodium hydroxide/ethanol mixture or 70% formamide to prepare chromatin fibers which they called "free DNA." Hybridization signals from cosmid probes appeared as extended lines and overlaps between clones were determined using the lengths of the probe signals and their known kilobase size as an internal standard. Typical experiments calculated averages from 30 or more signals (Senger et al. 1994).

Wiegant et al. (1992) and Lawrence et al. (1992) applied a different chemical method to release DNA from cells producing so-called "DNA halos." The procedure was based on detergent and high salt extraction followed by intercalating dye/UV treatment (Cook et al. 1976; Vogelstein et al. 1980). Using multicolor hybridizations, these investigators were able to determine relative map positions and to detect 10-kb overlap between individual cosmid clones. Wiegant et al. (1992) noted cosmid-specific signals that appeared as linear beaded signals of about 10 μm (i.e., about 3.5–4 kb/μm), and the authors concluded that their DNA halo preparations produced "essentially linearized" DNA. The map configuration of α-satellite DNA arrays or single-copy DNA could typically be derived from analysis of only 5–10 cells. These findings were confirmed independently by the work of Lawrence et al. (1992). But as Gerdes et al. pointed out in their publication in 1994, "many procedures can be used to decondense DNA for in situ hybridization, however many of these result in highly variable and apparently random threads of DNA smeared erratically across the slide, with little if any retention of native morphology" (Gerdes et al. 1994). As the images in Figures 1D–1G illustrate, DNA halo preparations often show residual nuclei containing compact hybridization domains, while the direction, extent, and straightness of hybridization tracks on the extended chromatin appear to be highly variable.

If DNA molecules could be stretched uniformly in one direction, they might provide linear templates for visual FISH mapping. Parra and Windle (1993) described a procedure they termed "direct visual hybridization" (DIRVISH), in which 100–5000 cells in phosphate buffer were placed on a one end of a slide and air-dried. The slide was then immersed in a lysis solution containing detergent, removed after 5 min, and tilted to allow the drop of DNA to run down the slide. The procedure produced some linear arrangements of DNA but, on the basis of the extent of hybridization signals, the authors estimated that the DNA was extended to a length ranging from 40% to 200% of the length of relaxed duplex DNA, i.e., 3.4 nm/bp (Parra and Windle 1993).

In the following year, Heiskanen et al. (1994) published a protocol to stretch genomic DNA embedded in agarose. The DNA was melted on a microscope

Figure 2 Packaging of DNA into chromatin and chromosomes. Several levels of packing of DNA can be discriminated. Two-nanometer-wide DNA molecules are folded into 11-nm chromatin segments which, when tightly packed with nucleosomes, appear as 30-nm chromatin fibers. Further packing leads to chromosomal sections with a diameter of about 300 nm and the 700-nm-thick chromatids of metaphase chromosomes.
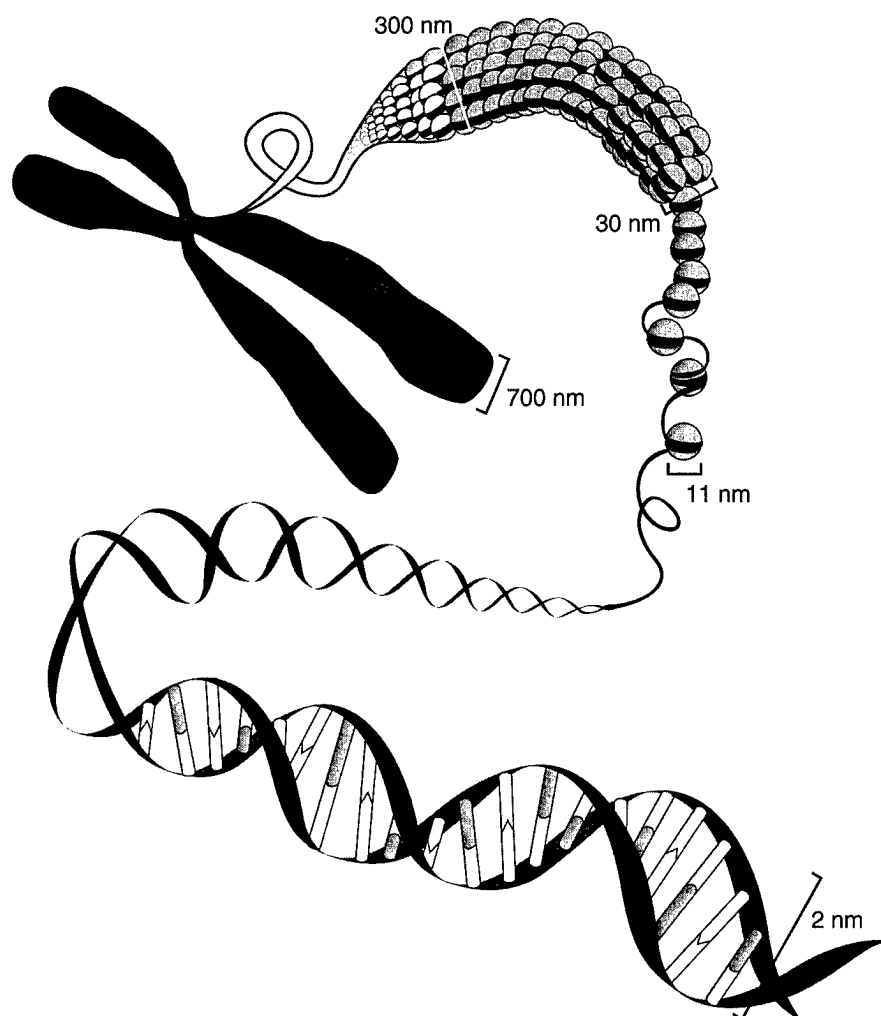
slide by heating the slide, then distributed and stretched manually using a coverslip. Major drawbacks of this manual procedure were heterogeneous stretching and a rather low abundance of informative signals on the slides.

Procedures published by 1995 allowed FISH for most preparations of decondensed nuclear or isolated cloned DNA and visualization of probe overlap to provide some information about the existence and size of gaps between clones (Parra and Windle 1993; Florijn et al. 1995; Heiskanen et al. 1995,1996). However, none of these techniques provided sufficiently accurate information about the extent of clone overlap or the separation between elements in the map because the chromatin onto which clones were mapped was condensed to various degrees from site to site in these preparations (Rosenberg et al. 1995).

We demonstrated that cloned DNA fragments can readily be mapped by FISH onto DNA molecules straightened by the hydrodynamic action of a receding meniscus and, referring to its quantitative nature, we termed our technique "Quantitative DNA Fiber Mapping (QDFM)" (Weier et al. 1995). In QDFM, a solution of purified DNA molecules is placed on a flat surface prepared so that the DNA molecules slowly attach at one or both ends. The DNA solution is then spread over a larger area by placing a coverslip on top. DNA molecules are allowed to bind to the surface. During drying, the molecules are straightened and uniformly stretched by the hydrodynamic action of the receding meniscus. Molecules prepared in this manner are stretched with remarkable homogeneity. We estimated that a properly stretched molecule should extend about ~2.3 kb/μm, i.e., approximately 30% over the length predicted for a double-stranded DNA molecule of the same size (Bensimon et al. 1994; Weier et al. 1995) (Figure 1H). We also showed that QDFM can be applied to linear or circular DNA molecules ranging in size from a few kb to more than 1 Mbp, which enabled us to determine clone overlaps or to

map small probes with near-kilobase resolution onto entire yeast chromosomes and mega-YAC clones from the CEPH/Genethon library (Wang et al. 1996) (Figures 1J–1K).

The subsequent studies of Hu et al. (1996) and Yokota et al. (1997) presented rapid protocols to prepare DNA fibers on 3-aminopropyl-triethoxysilane-coated glass or mica slides. In their studies imaging λ DNA molecules by atomic force microscopy, Hu et al. (1996) let coverslipped DNA molecules bind to the surface for only a few minutes. When the coverslip was removed for imaging, the molecules were straightened by the moving meniscus. Yokota et al. (1997) developed a protocol in which the meniscus motion was controlled mechanically, which provided advantages in speed and uniformity of the straightened molecules.

Overcoming Challenges in Mapping Tandemly Repeated DNA Sequences

Most mammalian genomes contain very large blocks of heterochromatin. Certain regions such as the (near)-centromeric heterochromatin seem to be involved in karyokinesis and chromosome association during meiosis (Dozortsev et al. 2000), but the overall role of these clusters of "junk DNA" remains largely unknown (Epplen et al. 1998). Physical map assembly in heterochromatic regions by more conventional methods, i.e., clone fingerprinting or STS content mapping, has proved less efficient, and initial releases of maps of the human, *Drosophila*, and other complex genomes might suffer from the presence of major gaps.

Several groups applied DNA fiber mapping techniques to investigate the interface between euchromatic and heterochromatic regions as well as the organization of tandem DNA repeats in humans (Wiegant et al. 1992; Haaf and Ward 1994b; Shiels et al. 1997), animals (Sjöberg et al. 1997; Li et al. 2000), and plants (Fransz et al. 1996; Jackson et al 1998,1999; Zhong et al. 1998). The methods applied by these researchers ranged from DNA halo preparations and extended chromatin to highly purified DNA molecules. Published results showed very specific beads-on-a-string patterns and presented convincing cases that DNA fiber mapping is a powerful tool to decipher the organization and extent of centromeric and telomeric DNA repeats.

Mapping of Single-copy DNA

Physical Map Assembly

The assembly of high-resolution physical maps has been a major application of DNA fiber mapping. Successful efforts to construct local maps for delineation of disease genes were mentioned above, but the suc-cess of additional investigators deserves proper recognition.

Klockars et al. (1996) used fiber–FISH to construct a physical map of the CLN5 region on 13q22. Duell et al. (1997,1998) constructed high-resolution physical maps based on QDFM for the immunoglobulin-β region on chromosome 22 and a large region including the 5' end of the human apolipoprotein B gene on chromosome 2. Theuns et al. (1999) determined the genomic organization of the human presenilin 1 gene, which was localized on chromosome 14q24.3, by fiber–FISH. Although applying different techniques to prepare the DNA fibers, these recent applications of DNA fiber mapping were able to support ongoing mapping efforts by providing physical maps with near-kilobase resolution.

Direct Visualization of Gene Amplifications and Deletions

Linearly extended chromatin or DNA molecules are ideal substrates to study gene amplification or deletions. Parra and Windle (1993) applied the DIRVISH technique to resolve low level amplifications of the dihydrofolate reductase (DHFR) gene in a hamster cell line. All DNA fiber mapping procedures are single DNA molecule investigations, which permit study of cell-to-cell variations. Parra and Windle (1993) presented evidence that DIRVISH can resolve the diversity in structure and complexity found in the amplified DHFR array, which would normally escape detection and proper characterization.

Michalet et al. (1997) extended human genomic DNA on silanized glass surfaces using a receding meniscus and found that a precise measurement of hybridized DNA probes can be achieved without normalization. Stretching yeast genomic DNA amounts representing hundreds of eukaryotic genomes, the authors performed the high-resolution mapping of cosmid contigs on a yeast artificial chromosome (YAC). Furthermore, stretching of human genomic DNA allowed measurement of gaps between contigs and determination of microdeletions in the tuberous sclerosis 2 gene of patients' DNA.

Mapping of Expressed Sequences

Applications of DNA fiber mapping extend beyond map assembly and can provide valuable information for clone validation, definition of a minimal tiling path, and quality control in the sequence assembly process. Even more exciting, its high hybridization efficiency makes DNA fiber mapping the method of choice for visual mapping of expressed sequences.

Several approaches exist to map expressed sequences or to study the organization of larger genes.

Gene fragments or entire cDNAs cloned in plasmid vectors can be amplified by in vitro DNA amplification using the polymerase chain reaction (PCR), labeled with reporter molecules, and used as hybridization probes (Wang et al. 1996). Figure 1 shows two examples of this application. A cloned cDNA fragment containing exon 2 of the human protein 4.1 gene (Peters et al. 1998) (Figure 1I) was positioned accurately on a closed circular, co-linear BAC DNA molecule. Counterstaining the BAC vector part with a combination of FITC- and digoxigenin-labeled probes that were detected in green and red, respectively, the position of gene 4.1 exon 2 within the BAC insert (the red signal on top of blue counterstain) can be determined with near-kilobase resolution.

The organization of genes in transcribed sequences interrupted by intronic sequences can be easily demonstrated by DNA fiber–FISH. We used QDFM in an attempt to resolve the structure of a gene from chromosome 20 frequently found amplified in human tumors (Tanner et al. 1994). As Figure 1L shows, a cDNA clone of about 5 kb maps to three distinct positions on a co-linear BAC clone. This result should be considered a rough estimate because exons smaller than 500 bp may not be detectable with this simple method (Weier et al. 1995). On the other hand, QDFM mapping turned out to be a highly reproducible method, so that was sufficient to analyze no more than five to eight BAC molecules (Weier 2001).

Technical developments in recent years have opened the doors to mapping of even smaller exons. In 1996, Florijn et al. demonstrated the use of DNA halo preps for mapping of exons ranging in size from 202 to 778 bp. Co-hybridization of co-linear cosmid clones enabled this group to reproducibly locate exon fragments of about 200 bp on extended genomic DNA in the context of the cognate cosmid signal. Detection efficiencies of 70–90% were found with probes larger than 400 bp, but the detection efficiency decreased to about 30% when fragments of about 200–250 bp were mapped.

More recently, Aaltonen and co-workers (1997; Horelli–Kuitunen et al. 1999) used a tyramide-based method (Raap et al. 1995) for detection of small hybridization targets. By applying this sensitive detection scheme to create a visual transcript map of six genes on chromosome 21q22.3, Horelli–Kuitunen et al. (1999) were able to detect targets ranging from 316 to 956 bp on 25–44% of the fibers. Independent experiments confirmed that an average of 89% of the EST hybridization signals were specific signals. These results suggested that a mere increase in detection sensitivity may not be sufficient to significantly increase the success rates of DNA fiber mapping experiments, i.e., the overall efficiency of hybridization and detection.

In the experiments conducted by Horelli–Kuitunen et al. (1999), the DNA fibers were prepared from agarose-embedded human genomic lymphocyte chromatin according to the protocol of Heiskanen et al. (1994,1995), which may have limited the access of probes and detection reagents to the target DNA. As van der Rijke et al. (2000) proposed, the loss of target DNA and limited accessibility due to in situ renaturation and attachment might have a negative impact on the detection efficiency. In the author's opinion, DNA fiber–FISH sensitivity is determined by hybridization efficiency, rather than the ability to generate sufficient signal from small probes (van der Rijke et al. 2000).

High-resolution Studies of DNA Replication

Despite intense efforts, the orderly activation of replication sites in genomes of higher organisms remains largely unexplained. The main reason for this may be the complexity of a process orchestrating the partly parallel activation of an estimated 10^4 to 10^6 replication sites.

DNA fiber mapping, with its high resolution and sensitivity, might provide important mapping information about the location and spacing of replication sites. Several groups used fiber mapping techniques to demonstrate replication forks in yeast (Rosenberg et al. 1995), in *Xenopus laevis* (Herrick et al. 2000), and in humans (Gerdes et al. 1994; Haaf 1996). The approach chosen by Rosenberg et al. (1995) was based on the previously described DIRVISH and DNA halo techniques (Wiegant et al. 1992; Parra and Windle 1993). Hybridizing differentially labeled cosmid probes to yeast and YAC DNA fibers, the authors could provide convincing visual evidence of DNA replication "forks" and "eyes" in YACs containing human DNA (Rosenberg et al. 1995). A rather limited number of experiments enabled the authors to identify two origins of replication in a 400-kb region containing the human dystrophin gene, to present evidence for bi-directional replication and to demonstrate that human DNA cloned in yeast is capable of initiating its own replication.

Studies described by Gerdes et al. (1994), Haaf (1996), and Herrick et al. (2000) used incorporation of non-isotopically labeled nucleotides as markers for replicated DNA. The results of Gerdes et al. (1994) showed pulse-incorporated bromodeoxyuridine (BrdU) representing nascent replicating DNA localized with the base of the chromatin loops in halo preparations. At increasing chase times, the replicated DNA was consistently found farther out on the extended region of the halo (Gerdes et al. 1994). Haaf (1996) investigated the timing of replication of α-satellite DNA arrays by incorporation of BrdU into newly synthesized DNA, followed by hybridization of biotinylated chromosome-specific alphoid probes to DNA released

from fibroblast or lymphoblast cell nuclei. Using the DNA halo preparations, he was able to demonstrate many independent replication sites within the large clusters of tandemly repeated alphoid DNA and partially hemizygous hybridization patterns in support of the hypothesis that replication of α-satellite DNA on homologous chromosomes is highly asynchronous.

The recent work of Herrick et al. (2000) extended previous applications of DNA fibers produced by the hydrodynamic action of a receding meniscus (Bensimon et al. 1994; Weier et al. 1995). *Xenopus* sperm nuclei were labeled by incorporation of biotin-dUTP in newly synthesized DNA followed by pulse-labeling with digoxigenin-dUTP at fixed time intervals. Because triphosphate deoxynucleosides do not efficiently traverse the intact cell membrane, all experiments had to be carried out with de-membranated sperm nuclei and activated egg extracts (Hyrien and Mechali 1992). Using red and green fluorescent antibodies directed against biotin and digoxigenin, respectively, the authors were able to discriminate early from late replicating sequences and to obtain estimates of the formation of new replication forks.

Conclusions

Recent research has lead to major improvements in hybridization-based physical mapping procedures. Developments in DNA fiber mapping have reached the point of immediate practical utility: DNA probes as small as 500 bp can be mapped routinely onto immobilized templates composed of linear or circular DNA molecules that range in size from less than 10 kb to more than one Mbp. Uniform stretching facilitates the conversion of measured physical distances into genomic distances. The highly reproducible stretching procedures require analysis of only a few DNA molecules for accurate determination of map positions by multicolor fluorescence microscopy and digital image analysis. A mapping accuracy in the kb range coupled to efficient signal amplification procedures to visualize signals from small targets allows rapid assembly of high-resolution physical maps for large-scale sequencing and map closure as well as high-resolution maps of expressed sequences.

DNA fiber mapping technologies will enhance performance of virtually all mapping and sequencing projects, including ongoing and future sequencing of model organisms and bacterial genomes. Implementation of these technologies will expedite sequencing by increasing parallelism, will lower the overall cost by reducing template redundancies, and will expedite map closure. Furthermore, the techniques will benefit the positional cloning of disease genes and characterization of genomic elements controlling their expression.

Literature Cited

Aaltonen J, Horelli–Kuitunen N, Fan JB, Bjorses P, Perheentupa J, Myers R, Palotie A, Peltonen L (1997) High-resolution physical and transcriptional mapping of the autoimmune polyendocrinopathy-candidiasis-ectodermal dystrophy locus on chromosome 21q22.3 by FISH. Genome Res 7:820–829

Aburatani H, Stanton VP, Housman DE (1996) High-resolution physical mapping by combined Alu-hybridization/PCR screening: construction of a yeast artificial chromosome map covering 31 centimorgans in 3p21-p14. Proc Natl Acad Sci USA 93:4474–4479

Ashworth LK, Batzer MA, Brandriff B, Branscomb E, de Jong P, Garcia E, Garnes JA, Gordon LA, Lamerdin JE, Lennon G, Mohrenweiser H, Olsen AS, Slezak T, Carrano AV (1995) An integrated metric physical map of human chromosome 19. Nature Genet 11:422–427

Bell C, Budarf ML, Nieuwenhuijsen BW, Barnoski BL, Buetow KH (1995) Integration of physical, breakpoint and genetic maps of chromosome 22. Localization of 587 yeast artificial chromosomes with 238 mapped markers. Hum Mol Genet 4:59–69

Bellanné-Chantelot C, Lacroix B, Ougen P, Billault A, Beaufils S, Bertrand S, Georges I, Glibert F, Gros I, Lucotte G, Susini L, Codani JJ, Gesnouin P, Pook S, Vaysseix G, Lu-Kuo J, Ried T, Ward D, Chumakov I, Le Paslier D, Barillot E, Cohen D (1992) Mapping the whole human genome by fingerprinting yeast artificial chromosomes. Cell 70:1059–1068

Bensimon A, Simon A, Chiffaudel A, Croquette V, Heslot F, Bensimon D (1994) Alignment and sensitive detection of DNA by a moving interface. Science 265:2096–2098

Brandriff B, Gordon L, Trask B (1991a) A new system for high-resolution DNA sequence mapping interphase pronuclei. Genomics 10:75–82

Brandriff BF, Gordon LA, Trask BJ (1991b) DNA sequence mapping by fluorescence in situ hybridization. Environ Mol Mutagen 18:259–262

Brandriff BF, Gordon LA, Tynan KT, Olsen AS, Mohrenweiser HW, Fertitta A, Carrano AV, Trask BJ (1992) Order and genomic distances among members of the carcinoembryonic antigen (CEA) gene family determined by fluorescence in situ hybridization. Genomics 12:773–779

Branscomb E, Slezak T, Pae R, Galas D, Carrano AV, Waterman M (1990) Optimizing restriction fragment fingerprinting methods for ordering large genomic libraries. Genomics 8:351–366

Cheng J-F, Weier H-UG (1997) Approaches to high resolution physical mapping of the human genome. In Fox CF, Connor TH, eds. Biotechnology International. San Francisco, Universal Medical Press, 149–157

Coffey AJ, Roberts RG, Green ED, Cole CG, Butler R, Anand R, Giannelli F, Bentley DR (1992) Construction of a 2.6-Mb contig in yeast artificial chromosomes spanning the human dystrophin gene using an STS-based approach. Genomics 12:474–484

Cohen D, Chumakov I, Weissenbach J (1993) A first-generation physical map of the human genome. Nature 366:698–701

Collins F, Galas D (1993) A new five-year plan for the U.S. human genome project. Science 262:43–46

Cook PR, Brazell IA, Jost E (1976) Characterization of nuclear structures containing superhelical DNA. J Cell Sci 22:303–324

Cox DR, Burmeister M, Price ER, Kim S, Myers RM (1990) Radiation hybrid mapping: a somatic cell genetic method for constructing high-resolution maps of mammalian chromosomes. Science 250:245–250

Dozortsev D, Coleman A, Nagy P, Diamond MP, Ermilov A, Weier U, Liyanage M, Ried T (2000) Nucleoli in a pronuclei-stage mouse embryo are represented by major satellite DNA of interconnecting chromosomes. Fertil Steril 73:366–371

Duell T, Nielsen LB, Jones A, Young SG, Weier H-UG (1998) Construction of two near-kilobase resolution restriction maps of the 5' regulatory region of the human apolipoprotein B gene by quantitative DNA fiber mapping (QDFM). Cytogenet Cell Genet 79:64–70

Duell T, Wang M, Wu J, Kim U-J, Weier H-UG (1997) High resolution physical map of the immunoglobulin lambda variant gene cluster assembled by quantitative DNA fiber mapping. Genomics 45:479–486

Epplen JT, Maueler W, Santos EJ (1998) On GATAGATA and other "junk" in the barren stretch of genomic desert. Cytogenet Cell Genet 80:75–82

Fidlerova H, Senger G, Kost M, Sanseau P, Sheer D (1994) Two simple procedures for releasing chromatin from routinely fixed cells for fluorescence in situ hybridization. Cytogenet Cell Genet 65:203–205

Florijn RJ, Bonden LAJ, Vrolijk H, Wiegant J, Vaandrager J-W, Baas F, den Dunnen JT, Tanke HJ, van Ommen G-JB, Raap AK (1995) High-resolution DNA fiber-FISH for genomic DNA mapping and colour bar-coding of large genes. Hum Mol Genet 4:831–836

Florijn RJ, van der Rijke FM, Vrolijk H, Blonden LA, Hofker MH, den Dunnen JT, Tanke HJ, van Ommen GJ, Raap AK (1996) Exon mapping by fiber-FISH or LR-PCR. Genomics 38:277–282

Fransz PF, Alonso–Blanco C, Liharska TB, Peeters AJM, Zabel P, de Jong JH (1996) High-resolution physical mapping in Arabidopsis thaliana and tomato by fluorescence in situ hybridization to extended DNA fibres. Plant J 9:421–430

Gerdes MG, Carter KC, Moen PT Jr, Lawrence JB (1994) Dynamic changes in the higher-level chromatin organization of specific sequences revealed by in situ hybridization to nuclear halos. J Cell Biol 126:289–304

Green ED, Mohr RM, Idol JR, Jones M, Buckingham JM, Deaven LL, Moyzis RK, Olson MV (1991) Systematic generation of sequence-tagged sites for physical mapping of human chromosomes application to the mapping of human chromosome 7 using yeast artificial chromosomes. Genomics 11:548–564

Green ED, Olson MV (1990) Systematic screening of yeast artificial-chromosome libraries by use of the polymerase chain reaction. Proc Natl Acad Sci USA 87:1213–1217

Haaf T (1996) High-resolution analysis of DNA replication in released chromatin fibers containing 5-bromodeoxyuridine. Biotechniques 21:1050–1054

Haaf T, Ward DC (1994a) High resolution ordering of YAC contigs using extended chromatin and chromosomes. Hum Mol Genet 3:629–633

Haaf T, Ward DC (1994b) Structural analysis of α-satellite DNA centromere proteins using extended chromatin and chromosomes. Hum Mol Genet 3:697–709

Heiskanen M, Hellsten E, Kallioniemi OP, Makela TP, Alitalo K, Peltonen L, Palotie A (1995) Visual mapping by fiber-FISH. Genomics 30:31–36

Heiskanen M, Kallioniemi O, Palotie A (1996) Fiber-FISH: experiences and a refined protocol. Genet Anal Biomol Eng 12:179–184

Heiskanen M, Karhu R, Hellsten E, Peltonen L, Kallioniemi OP, Palotie A (1994) High resolution mapping using fluorescence in situ hybridization to extended DNA fibers prepared from agarose-embedded cells. Biotechniques 17:928–933

Heng HHQ, Squire J, Tsui LC (1992) High-resolution mapping of mammalian genes by in situ hybridization to free chromatin. Proc Natl Acad Sci USA 89:9509–9513

Herrick J, Stanislawski P, Hyrien O, Bensimon A (2000) Replication fork density increases during DNA synthesis in X. laevis egg extracts. J Mol Biol 300:1133–1142

Hoheisel JD, Lehrach H (1993) Use of reference libraries and hybridisation fingerprinting for relational genome analysis. FEBS Lett 325:118–122

Horelli–Kuitunen N, Aaltonen J, Yaspo ML, Eeva M, Wessman M, Peltonen L, Palotie A (1999) Mapping ESTs by fiber-FISH. Genome Res 9:62–71

Hu J, Wang M, Weier HUG, Frantz P, Kolbe W, Olgletree DF, Salmeron M (1996) Imaging of single extended DNA molecules on flat (aminopropyl)triethoxysilane-mica by atomic force microscopy. Langmuir 12:1697–1700

Hyrien O, Mechali M (1992) Plasmid replication in xenopus eggs and egg extracts: a 2d gel electrophoretic analysis. Nucleic Acids Res 20:1463–1469

Ioannou PA, Amemiya CT, Garnes J, Kroisel PM, Shizuya H, Chen C, Batzer M, De Jong PJ (1994) A new bacteriophage P1-derived vector for the propagation of large human DNA fragments. Nature Genet 6:84–89

Jackson SA, Dong F, Jiang J (1999) Digital mapping of bacterial artificial chromosomes by fluorescence in situ hybridization. Plant J 17:581–587

Jackson SA, Wang ML, Goodman HM, Jiang J (1998) Application of fiber-FISH in physical mapping of Arabidopsis thaliana. Genome 41:566–572

Klockars T, Savukoski M, Isosomppi J, Laan M, Jarvela I, Petrukhin K, Palotie A, Peltonen L (1996) Efficient construction of a physical map by fiber-FISH of the CLN5 region: refined assignment and long-range contig covering the critical region on 13q22. Genomics 35:71–78

Lawrence JB, Carter KC, Gerdes MJ (1992) Extending the capabilities of interphase chromatin mapping. Nature Genet 2:171–172

Li Y, Lee C, Hsu TH, Li SY, Lin CC (2000) Direct visualization of the genomic distribution and organization of two cervid centromeric satellite DNA families. Cytogenet Cell Genet 89:192–198

Locke J, Rairdan G, McDermid H, Nash D, Pilgrim D, Bell J, Roy K, Hodgetts R (1996) Cross-screening: A new method to assemble clones rapidly and unambiguously into contigs. Genome Res 6:155–165

Lu-Kuo JM, Le Paslier D, Weissenbach J, Chumakov I, Cohen D, Ward DC (1994) Construction of a YAC contig and a STS map spanning at least seven megabasepairs in chromosome 5q34-35. Hum Mol Genet 3:99–106

Michalet X, Ekong R, Fougerousse F, Rousseaux S, Schurra C, Hornigold N, van Slegtenhorst M, Wolfe J, Povey S, Beckmann JS, Bensimon A (1997) Dynamic molecular combing: Stretching the whole human genome for high-resolution studies. Science 277:1518–1523

Nelson DL (1991) Applications of polymerase chain reaction methods in genome mapping. Curr Opin Genet Dev 1:62–68

Nizetic D, Gellen L, Hamvas RM, Mott R, Grigoriev A, Vatcheva R, Zehetner G, Yaspo ML, Dutriaux A, Lopes C, Delabar JM, Van Broeckhoven C, Potier MC, Lehrach H (1994) An integrated YAC-overlap and 'cosmid-pocket' map of the human chromosome 21. Hum Mol Genet 3:759–770

Olson MV (1993) The human genome project. Proc Natl Acad Sci USA 90:4338–4344

Parra I, Windle B (1993) High resolution visual mapping of stretched DNA by fluorescent hybridization. Nature Genet 5:17–21

Patil N, Peterson A, Rothman A, DeJong PJ, Myers RM, Cox DR (1994) A high resolution physical map of 2.5 Mbp of the Down syndrome region on chromosome 21. Hum Mol Genet 3:1811–1817

Peters LL, Weier HU, Walensky LD, Snyder SH, Parra M, Mohandas N, Conboy JG (1998) Four paralogous protein 4.1 genes map to distinct chromosomes in mouse and human. Genomics 54:348–350

Pierce JC, Sauer B, Sternberg N (1992) A positive selection vector for cloning high molecular weight DNA by the bacteriophage-P1

system—improved cloning efficacy. Proc Natl Acad Sci USA 89:2056–2060

Raap AK, van de Corput MP, Vervenne RA, van Gijlswijk RP, Tanke HJ, Wiegant J (1995) Ultra-sensitive FISH using peroxidase-mediated deposition of biotin- or fluorochrome tyramides. Hum Mol Genet 4:529–534

Rosenberg C, Florijn RJ, Van der Rijke FM, Blonden LA, Raap TK, Van Ommen GJ, den Dunnen JT (1995) High resolution DNA fiber-FISH on yeast artificial chromosomes: direct visualization of DNA replication. Nature Genet 10:477–479

Sapolsky RJ, Lipshutz RJ (1996) Mapping genomic library clones using oligonucleotide arrays. Genomics 33:445–456

Selleri L, Eubanks JH, Giovannini M, Hermanson GG, Romo A, Djabali M, Maurer S, McElligott DL, Smith MW, Evans GA (1992) Detection and characterization of "chimeric" yeast artificial chromosome clones by fluorescent in situ suppression hybridization. Genomics 14:536–541

Senger G, Jones TA, Fidlerova H, Sanseau P, Trowsdale J, Duff M, Sheer D (1994) Released chromatin: linearized DNA for high resolution fluorescence in situ hybridization. Hum Mol Genet 3:1275–1280

Shiels C, Coutelle C, Huxley C (1997) Analysis of ribosomal and alphoid repetitive DNA by fiber-FISH. Cytogenet Cell Genet 76:20–22

Shizuya H, Birren B, Kim UJ, Mancino V, Slepak T, Tachiiri Y, Simon M (1992) Cloning and stable maintenance of 300-kilobase-pair fragments of human DNA in Escherichia coli using an F-factor-based vector. Proc Natl Acad Sci USA 89:8794–8797

Sjöberg A, Peelman LJ, Chowdhary BP (1997) Application of three different methods to analyse fibre-fish results obtained using four lambda clones from the porcine MHC III region. Chromosome Res 5:247–253

Stallings RL, Doggett NA, Callen D, Apostolou S, Chen LZ, Nancarrow JK, Whitmore SA, Harris P, Michison H, Breuning M, Saris JJ, Fickett J, Cinkosky M, Torney DC, Hildebrand CE, Moyzis RK (1992) Evaluation of a cosmid contig physical map of human chromosome 16. Genomics 13:1031–1039

Tanner M, Tirkkonon A, Kallioniemi A, Collins C, Stokke T, Karhu R, Kowbel D, Shadravan F, Hintz M, Kuo W-L, Waldman F, Isola J, Gray JW, Kallioniemi O-P (1994) Increased copy number at 20q13 in breast cancer defining the critical region: exclusion of candidate genes. Cancer Res 54:4257–4260

Theuns J, Cruts M, Del-Favero J, Goossens D, Dauwerse H, Wehnert A, den Dunnen JT, Van Broeckhoven C (1999) Determination of the genomic organization of human presenilin 1 by fiber-fish analysis and restriction mapping of cloned DNA. Mammal Genome 10:410–414

Trask B, Pinkel D, van den Engh G (1989) The proximity of DNA sequences in interphase cell nuclei is correlated to genomic distance and permits ordering of cosmids spanning 250 kilobase pairs. Genomics 5:710–717

Tynan K, Olsen A, Trask B, de Jong P, Thompson J, Zimmermann W, Carrano A, Mohrenweiser H (1992) Assembly and analysis of cosmid contigs in the CEA-gene family region of human chromosome 19. Nucleic Acids Res 20:1629–1636

van der Rijke FM, Florijn RJ, Tanke HJ, Raap AK (2000) DNA fiber-FISH staining mechanism. J Histochem Cytochem 48:743–745

Vetrie D, Bobrow M, Harris A (1993) Construction of a 5.2-megabase physical map of the human X chromosome at Xq22 using pulsed-field gel electrophoresis and yeast artificial chromosomes. Genomics 15:631–642

Vogelstein B, Pardoll DM, Coffey DS (1980) Supercoiled loops and eucaryotic DNA replication. Cell 22:79–85

Wang M, Duell T, Gray JW, Weier H-UG (1996) High sensitivity, high resolution physical mapping by fluorescence in situ hybridization on to individual straightened DNA molecules. Bioimaging 4:1–11

Waterston R, Sulston J (1995) The genome of Caenorhabditis elegans. Proc Natl Acad Sci USA 92:10836–10840

Weier H-UG (2001) Quantitative DNA Fiber Mapping. In Darzynkiewicz Z, Chrissman HA, Robinson JP, eds. Methods in Cell Biology. Vol 64. Part B. San Diego, Academic Press, 33–53

Weier H-UG, Wang M, Mullikin JC, Zhu Y, Cheng J-F, Greulich KM, Bensimon A, Gray JW (1995) Quantitative DNA fiber mapping. Hum Mol Genet 4:1903–1910

Weissenbach J, Gyapay G, Dib C, Vignal A, Morissette J, Millasseau P, Vaysseix G, Lathrop M (1992) A second-generation linkage map of the human genome. Nature 359:794–801

Wiegant J, Kalle W, Mullenders L, Brookes S, Hoovers JM, Dauwerse JG, van Ommen GJ, Raap AK (1992) High-resolution in situ hybridization using DNA halo preparations. Hum Mol Genet 1:587–591

Yokota H, Johnson F, Lu H, Robinson RM, Belu AM, Garrison MD, Ratner BD, Trask BJ, Miller DL (1997) A new method for straightening DNA molecules for optical restriction mapping. Nucleic Acids Res 25:1064–1070

Zhong XB, Fransz PF, Wennekes–Eden J, Ramanna MS, van Kammen A, Zabel P, Hans de Jong J (1998) FISH studies reveal the molecular and chromosomal organization of individual telomere domains in tomato. Plant J 13:507–517

Zucchi I, Schlessinger D (1992) Distribution of moderately repetitive sequences pTR5 and LF1 in Xq24-q28 human DNA and their use in assembling YAC contigs. Genomics 12:264–275